THREE DIMENSIONAL ANALYSIS OF EXTRUSION THROUGH TAPER DIE

A THESIS SUBMITTED IN PARTIAL FULFILMENT OF THE REQUIREMENTS FOR THE DEGREE OF

Master of Technology

in

Mechanical Engineering

By

Mithun Kumar Murmu

Department of Mechanical Engineering
National Institute of Technology
Rourkela MAY, 2009

THREE DIMENSIONAL ANALYSIS OF EXTRUSION THROUGH TAPER DIE

A THESIS SUBMITTED IN PARTIAL FULFILMENT OF THE

REQUIREMENTS FOR THE DEGREE OF

Master of Technology

in

Mechanical Engineering

[Specialization: Production Engineering]

By

Mithun Kumar Murmu

Under the Guidance of

Dr. Susanta Kumar Sahoo

Department of Mechanical Engineering

Department of Mechanical Engineering
National Institute of Technology

Rourkela

May, 2009

NATIONAL INSTITUTE OF TECHNOLOGY
ROURKELA – 769008
INDIA

CERTIFICATE

This is to certify that the thesis entitled, **"Three Dimensional Analysis of Extrusion Through Taper Die"** submitted by **Mithun Kumar Murmur** in partial fulfillment of the requirement for the award of **Master of Technology** Degree in **Mechanical Engineering** with specialization in Production Engineering at the National Institute of Technology, Rourkela (Deemed University) is an authentic work carried out by him under my supervision and guidance.

To the best of my knowledge, the matter embodied in the thesis has not been submitted to any other University/ Institute for the award of any degree or diploma.

Date:

Dr. Susanta Kumar Sahoo
Department of Mechanical Engineering
National Institute of Technology
Rourkela – 769008

NATIONAL INSTITUTE OF TECHNOLOGY
ROURKELA – 769008
INDIA

ACKNOWLEDGEMENT

I avail this opportunity to extend my hearty indebtedness to my guide **Dr.S.K.Sahoo**, Professor, Mechanical Engineering for his valuable guidance constant encouragement and kind help at different stages for the execution of this dissertation work.I am extremely thankful to **Prof. R. K. Sahoo** Head, Department of Mechanical Engineering and **Prof. S.S. Mohapatra**, Course Coordinator for their help and advice during the course of this work.

I am also thankful to **Mr.Y.Ali,** Technical assistant of cental workshop for their help during the execution of experiment. My friends **Shuvransu, L. N. Patra(Ph D Scholar)** and **Sontosh sahoo** deserve my special thanks for their help and support throughout this work.

I am also thankful to all my well wishers, class mates and friends for their inspiration and help.

Date :- 25/05/09

Mithun Kr Murmu.
Mithun Kumar Murmu
Roll No.-207ME202

ABSTRACT

An upper bound solution for extrusion of “triangular” sectioned product through taper die from round sectioned billet has been developed. A simple discontinuous kinematically admissible velocity field with optimization parameter is proposed. From the proposed velocity field the upper bound solution on non-dimensional extrusion pressure are determined with respect to chosen process parameters. The theoretical results are compared with experimental result to check the validity of the proposed velocity fields.

The reformulated SERR technique is used to find out the kinematically admissible velocity field applied to deformation zone surrounded by flat surfaces. This velocity field is used to compute upper bound extrusion pressure at various area of reduction.

The triangular sectioned product from round sectioned billet through taper die is taken for upper bound analysis using SERR technique. As this section is symmetry about one axis with round sectioned billet only one half of section is taken as domain interest for deformation zone to calculate the velocity field. Detailed formulations of models are presented.

To validate the proposed model/analysis experiments are carried out taking lead as the working material. An experimental set-up is designed and fabricated with four split type taper dies for this purpose. Experiments are carried out at dry and lubricated condition of the dies to check the friction effect.

The results obtained indicate that the predictions both in extrusion load and the deformed configuration are in good agreement with the experiment under different lubrication conditions.

CONTENTS

****

LIST OF FIGURES

NOMENCLATURE

J = Upper bound energy consumption

J_1 = Internal power of deformation

J_2 = Power of shear deformation

J_3 = Frictional power

σ_0 = Yield stress in uniaxial tension

ε_{ij} = Components of strain tensor

V = Volume of deformation zone

Si = The surface of velocity discontinuity

Sj = The surface of die/work

$|\nabla V|_{Si}$ = Velocity discontinuity along with surface

$|\nabla V|_{Sj}$ = Velocity discontinuity along Sj surface

$\overset{\Lambda}{n}$ = Unit normal vector

a = half width

L = Optimization parameter

W = Half width of billet

Vx ,Vy, Vz = Components of velocity in Cartesian co-opdinate

V_b = Billet velocity

V_P = Product velocity

J_{MIN} = Minimum value of upper bound energy consumption

R = Radius of billet

N = Number of sides

L = Length of deformation zone

H = Height of the triangle(of triangular section)

B = Side of triangle

X,Y Z = Axis of general cartesianco-ordinate

A x, Ay, Az = Area of X, Y, Z projection of triangle in space

P_{avg} = avg pressurwe.

CHAPTER ONE

INTRODUCTION

CHAPTER 1

1.1 INTRODUCTION

Extrusion is an often-used forming process among the different metal forming operations and its industrial history dates back to the 18th century. A billet is placed in the container and pressed by the punch, causing the metal to flow through a die with an opening. In the process of extrusion, a billet is placed in an enclosed chamber. The chamber has an opening through which the excess material escapes as the volume of chamber is reduced when pushed by ram. The escaped material has a uniform cross section identical with that of the opening. In general extrusion is used to produce cylindrical bars or hollow tubes. A large variety of irregular cross sections are also produced by this process using dies of complex shapes. The process has definite advantage over rolling for production of complicated section having re-entrant corners. In this process large reduction achieved even at high strain rates has made it one of the fastest growing metal working methods.

Because of large force required in extrusion most metals are extruded hot when the deformation resistance of metal is low. However cold extrusion is also possible for many metals and has become an important commercial process. The reaction of the billet with the container and the die results in high compressive stresses that effectively reduce cracking of materials during primary breakdown from ingot. This is an important reason for increased commercial adoption of extrusion in the working of metals difficult to form such as stainless steel, nickel, nickel based alloys and other high temperature materials.

More than ten years ago, researchers started to be attracted by three-dimensional problems in metal forming. Today three-dimensional modeling is still regarded as a highlighted and difficult problem. Different methods of analysis have been extended to three dimensional, among which the finite element analysis is most commonly used. Most of the results that have

been published on three dimensional finite element method simulations are based on different software package like DEFORM-3D (ALGOR).

1.2 Metal Forming

Forming is defined as the plastic deformation of a billet between tools (dies) to obtain the final configuration. It may be classified roughly into five categories: mechanical working, such as forging, extrusion rolling, drawing, and various sheets forming process; casting; powder and fiber metal forming; and joining process. Forming is generally employed for those components, which require high strength, high resistance to shock and vibration, and uniform properties.

With the rapid advancement of new technologies like aerospace, aircraft, missile and automobile, the need for light and high strength, anti corrosion products are observed. Now a day the main constrain is the amount material resources, which is depleting at an alarming rate. So considering all the aspects, industries mostly depend on metal forming operations to minimize the material losses. The advantages of metal forming processes are:

1.The desired size and shape are obtained through the plastic deformation of materials.
2. It's a very economical process where the desired size, shape and surface can be obtained without any significance loss of material.
3. The input energy can be fruitfully utilized in improving the strength.
4. Strain and hardness are increased due to strain hardening.

1.3 Extrusion Process

The forcing of solid metal through a suitably shaped orifice under compressive forces. Extrusion is somewhat analogous to squeezing toothpaste through a tube, although some cold extrusion processes more nearly resemble forging, which also deforms metals by application of compressive forces. Most metals can be extruded, although the process may not be economically feasible for high-strength alloys. The most widely used method for producing extruded shapes is the direct, hot extrusion process. In this process, a heated billet of metal is placed in a cylindrical chamber and then compressed by a hydraulically operated ram. The

extrusion of cold metal is variously termed cold pressing, cold forging, cold extrusion forging, extrusion pressing, and impact extrusion. The term cold extrusion has become popular in the steel fabrication industry, while impact extrusion is more widely used in the nonferrous field. Advantages of cold extrusion are higher strength because of severe strain-hardening, good finish and dimensional accuracy, and economy due to fewer operations and minimum of machining require.

The extrusion process is basically classified into three categories according to the flow direction in relation to the punch movement. This classification is namely forward, backward and impact extrusion.

1.3.1 Forward Extrusion

Forward extrusion, reduces slug diameter while increasing length. Metal flows same direction to the ram. Stepped shafts and cylinders are typical examples of this process.

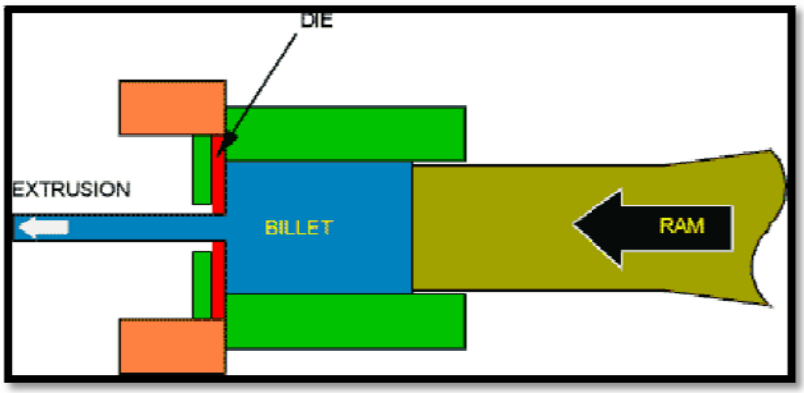

Fig.1.1 Forward extrusion

1.3.2 Backward extrusion

Backward extrusion produces hollow parts. Here, the metal flows back around the descending ram in the opposite direction.

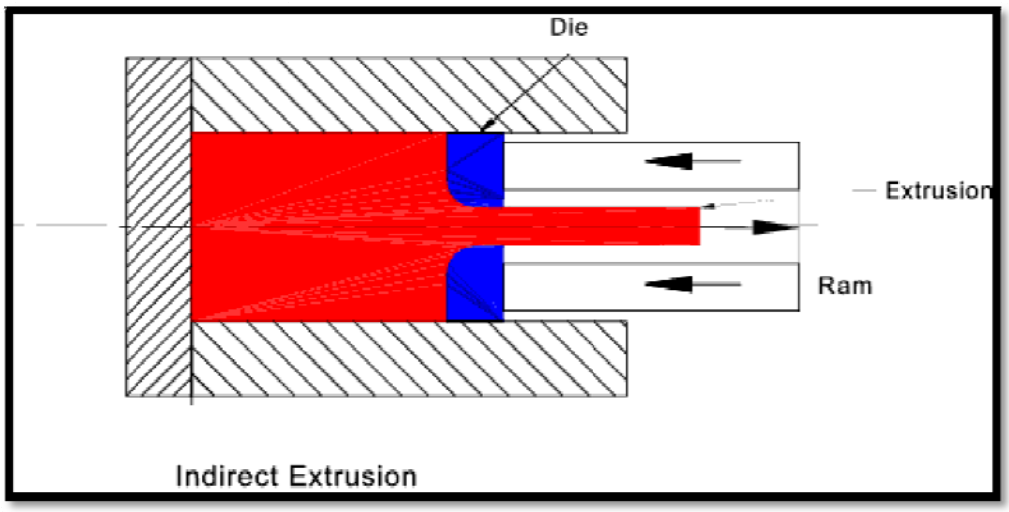

Fig. 1.2 Backward extrusion

1.3.3 Impact extrusion

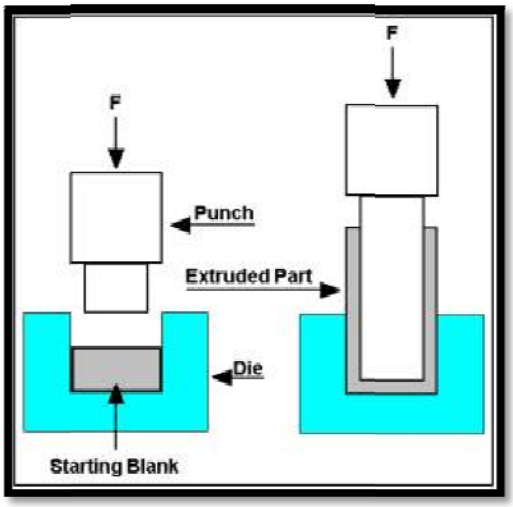

Fig. 1.3 Impact Extrusion

Advantages Extrusion processes are:

1. The desired size and shape are obtained through the plastic deformation of material.

2. it's a very economical process where the desired size, shape and surface finish can be obtained without any significance loss of material.

3. The input energy can be fruitfully utilized in improving the strength.

4. Strain and hardness are increased due to strain hardening.

Among the different metal forming processes, extrusion has definite advantages over others for the production of three dimensional section shapes. Now it is becoming essential to pay greater attention to the extrusion of section rod from round stock, as this operation offers the promises of an economic production route. The process is also attractive because press machines are readily available and the necessity to purchase expensive section stock corresponding to a multiplicity of required sections is eliminated.

The analysis of the stresses in the metal working process has been an important area of plasticity for the past few years. Since the forces and the deformations generally are quite complex.

It is usually useful to use simplifying assumptions to obtain a traceable solution. The principal use of analytical study of metalworking process is for determining the forces required to produce a given deformation for a certain geometry prescribed by the process and is the ability to make an accurate prediction of the stress, strain, and velocity at every point in the deformed region of the work piece.

For the extrusion of sections, converging dies with lubricants are more preferred to flat dies, as the former provide a gradual change in shape and reduction of area simultaneously. The flat-faced or square die has the disadvantage of not providing any work hardening effect, thus requiring high extrusion energy.

The upper-bound technique appears to be a useful tool for analyzing 3D metal forming problems when the objective of such an analysis is limited to prediction of the deformation

load and study of metal flow during the process. This is so because the classical slip line field solution is not applicable to this class of problem and the finite element method (FEM) is constrained by computational difficulties to achieve accuracy in these cases.

Different methods are there to solve the metal forming problems

1. Severity solution
2. Slip line solution
3. Upper bound solution
4. Lower bound solution
5. Finite element analysis

1.4 Upper bound solution.

An upper bound analysis provides an overestimation of the required deformation force. It is more accurate because it will always result in an overestimation of the load that the press or the machine will be called upon to deliver. In this case factor of safety will be automatically built in. In this analysis, the deformation is assumed to take place by rigid body movement of triangular blocks in which all particles in a given element moves with the some velocity.

A kinematically admissible velocity should satisfy the

- Continuity equation
- Velocity boundary condition
- Volume constancy condition

The power of deformation calculated from this is higher than the actual one, called upper bound. When applying upper bound, the first step is to conceive of a velocity field for the deforming body.

- The field can be easily imagined and related to our visual experience.
- Velocity can be measured directly and is easily displayed in a physical manner.
- In this case factor of safety is automatically in built
- It is comparatively easy to analyze.

There exists an infinite no stress field that satisfy the prescribed condition for a lower bound solution and an infinite number of velocity that satisfy the upper bound condition. It is generally assumed that velocity field that the highest lower bound that provides the highest lower bound is closest in characteristics to the actual velocity. Likewise, generally assume a stress field that provides highest lower bound the closest to the actual stress distribution.

Theoretical consideration of this process has been neglected as simple analytical techniques can not yield valid relationships. Therefore, it has been very difficult to determine the appropriate working conditions of extrusion and to design the optimum die shape and dimensions for the required product. For a long time, those matters have been based on empirical knowledge.

1.4 LITERATURE REVIEW

Now it is becoming essential to pay greater attention to the extrusion of section rod from round stock, as this operation offers the promise of an economic production route. Despite the advantage of converging dies, only a few theoretical approaches to the extrusion or drawing processes for 3D shapes have been published.
Nagpal and Altan (1) introduced the concept of dual stream functions to express 3D flow in the die and analyzed the force of extrusion from round billet to elliptical bars.
Basily and Sansome (2)made an upper-bound analysis of drawing of square sections from round billets by using triangular elements at entry and exit of the die.

Yang and Lee (3) proposed kinematically admissible velocity fields for the extrusion of billets having generalized cross-sections, where the similarity in the profile of cross-section was assumed to be maintained throughout deformation. They analyzed the extrusion of polynomial billet with rectilinear and curvilinear sides.

Johnson and Kudo (4) have proposed upper bound for plain strain axis-symmetry extrusion, for extrusion through smooth square dies. in this case materials was assumed to be rigid, perfectly plastic and work hardening effect being neglected.

Hill et al.(5) proposed the first genuine attempt to develop a general method of analysis of three dimensional metal deformation problem choosing a class of velocity field that nearly satisfies the statistically requirements, by using the virtual work principle for the continuum.

Prakash and Khan (6) made an upper-bound analysis of extrusion and drawing through dies of polygonal cross-sections with straight stream lines, where the similarity in shape was maintained. The upper-bound technique appears to be a useful tool for analyzing 3D metal forming problems when the objective of such an analysis is limited to prediction of the deformation load and study of metal flow during the process.

A method employing a discontinuous velocity field was proposed by Gatto and Giarda (7). This method is based on discretizing the deformation zone into elementary rigid regions. In such a scenario, the rigid regions have a constant internal velocity vector and the deformation

is assumed to occur at the interfaces of these regions. The rigid element assumption limits the use of this technique to problems with flat boundaries. Formulation appears suitable for problems where billet and product sections are similar.

P.K. Kar and N.S Das (8) modified this technique to solve problems with dissimilar billet and product sections. However, their formulation was also limited to problems with flat boundaries and, as such; the analysis of extrusion from round billets is excluded from their formulation.

However P.K. Kar and S.K. Sahoo (9) used the reformulated spatial elementary rigid region (SERR) technique for the analysis of round-to-square extrusion by approximating the circle into a polygon and successively increasing the number of sides of this approximating polygon until the extrusion pressure converged by using tapper dies

S.K. Sahoo a, P.K. Kar and K.C. Singh a (10) also used the reformulated SERR technique for the analysis of round-to-hexagonal section, channel section, triangular section extrusion through converging dies.

Narayanasamy et al. (11) proposed an analytical method for designing the streamlined extrusion have the cosine profile and an upper bound analysis is proposed for the extrusion of circular section from circular billets.

Hosino and Gunasekara (12) made an upper bound solution for extrusion and drawing of square section from round billets through converging dies formed by an envelope of straight lines.

Boer et al. (13) applied the upper bound approach to drawing of square rods from round stock, by employing a method of co-ordinate transformation.

Kim et al. (14) proposed the velocity field, based on upper bound analysis, for the prediction of the extrusion load in the square die forward extrusion of circular shaped bars from regular polygonal billets.

1.5 OBJECTIVE OF THESIS

The objective of the work is to find an upper bound solution using three dimensional discontinuous kinematically admissible velocity field for the configuration under consideration.

1. To find out a class of kinematically admissible velocity discontinuous field based on the reformulated SERR technique.

2. To find the optimum velocity from velocity field.

3. Computation of upper bound extrusion pressure at various area reductions to get triangular section extruded product through taper die from round section billet using optimum velocity field.

4. Analysis of stresses distribution in the deformation process.

5. To design and develop an extrusion setup (Dies)

CHAPTER TWO

THEORETICAL ANALYSIS

CHAPTER 2

2.1 THEORETICAL ANALYSIS

For many metals working operation exact solution for the load to cause plastic deformation are either non-existent or too difficult to compute. The Upper bound solution is constructed on what is known as kinematically admissible velocity field. A velocity field is said to be kinematically admissible if it is consistent with the velocity boundary condition both in rigid as well as the plastic zone. Upper bound solution is the best method for calculating the extrusion pressure.

The principal use of analytical study of metalworking process is for determining the forces required to produce deformation for a certain geometry prescribed by the process and is the ability to make an accurate prediction of the stress, strain, and velocity at every point in the deformed region of the work piece. Since the calculation are useful for selecting or designing the equipment to do a particular job. While an analytical method is only possible if a sufficient number of boundary conditions are specified, the mathematical difficulties in general solutions are formidable. The most of analysis of actual metal working process is limited to two dimensional, symmetrical problems. Upper bound solution can be applied to three dimensional problems.

The formal statement of the upper-bound theorem is that the power of deformation calculated in kinematically admissible velocity fields, is greater than the actual. The power of deformation calculated from this is higher than the actual one, called upper bound. When applying upper bound, the first step is to conceive of a velocity field for the deforming body. An upper bound analysis provides an overestimation of the required deformation force. It is more accurate because it will always result in an overestimation of the load that the press or the machine will be called upon to deliver. In this analysis, the deformation is assumed to take place by rigid body movement of triangular blocks in which all particles in a given element moves with the some velocity. For continuum deforming plastically in contact with a die, the rate of energy dissipated, J, is given by

$$J=J_1+J_2+J_3 \quad \ldots\ldots\ldots\ldots\ldots\ldots \quad (2.1)$$

where

J_1 is the power dissipated for internal plastic deformation

J_2 is the power dissipated at surfaces of velocity discontinuity (shear deformation)

J_3 is the power dissipated due to friction at the die–work piece interface

For a material obeying Levy-Misses flow rule the internal power J1 is given by

$$J_1 = (2\sigma_0/\sqrt{3})\int_V [(1/2)\varepsilon_{ij}\varepsilon_{ij}]\,dv \quad \ldots\ldots\ldots\ldots \quad (2.2)$$

Where, σ_0 is the yield stress in uniaxial tension and ε_{ij} is the strain rate tensor. The internal Power is computed by integrating Von-Misses equation over total volume V_0.

$$\varepsilon_{ij} = 1/2\,[\partial V_i/\partial X_j + \partial V_j/\partial X_i] \quad \ldots\ldots\ldots\ldots\ldots\ldots \quad (2.3)$$

The power of shear deformation, J_2 along the velocity discontinuity surface S_i present in the deformation zone is given by,

$$J_2 = (\sigma_0/\sqrt{3})\int_{S_i} \left|\Delta V\right|_{S_i} dS_i \quad \ldots\ldots\ldots\ldots\ldots\ldots \quad (2.4)$$

The friction power J_3 is dissipated at the tool/work piece is determined from the relation

$$J_3 = (m\sigma_0/\sqrt{3})\int_{S_j} \left|\Delta V\right|_{S_j} dS_j \quad \ldots\ldots\ldots\ldots\ldots\ldots \quad (2.5)$$

Where m is the friction factor and $|\Delta V|_{si}$, $|\Delta V|_{Sj}$ are the magnitude of velocity discontinuity at the surfaces Si and Sj respectivel. If the kinematically admissible velocity field postulated for the forming process under consideration is the actual one, the power J calculated from equation (2.1) is the exact value. It is different from the actual equation (2.1) yields and upper bound to the power necessary for forming operation in question. .

2.2 SERR technique

The SERR technique is a method for analyzing there dimensional metal deformation problems was first proposed by Gotta and Giarda [5].The distinguishing feature of this technique is that the deformation zone is discretized into rigid regions thus providing a discontinuous velocity field in the deformation zone.

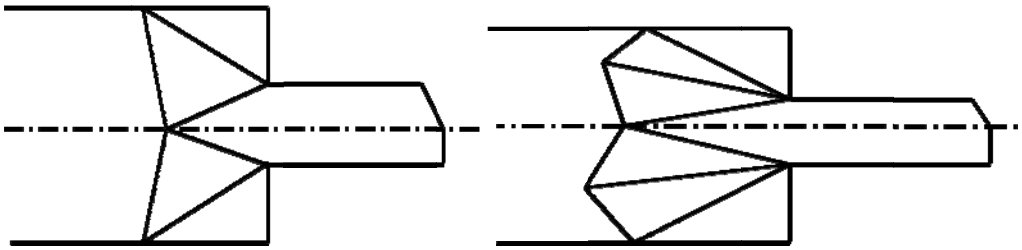

Fig.2.1 Jonhnson's Velocity Fig 2.2 Kudo's Velocity field

In plane strain solution, the velocity in a rigid region is determined when its components along two mutually perpendicular directions are known. Thus, the problem involves only two unknown and two equations necessary to determine them are obtained by considering the mass continuity condition on two faces bordering this rigid region. Hence the planner rigid region is always a triangle and this has formed the basis for the construction of the well known velocity fields by Johnson and Kudo shown in Fig 2.1 and Fig 2.2 for plane strain extrusion. In a three dimensional deformation problem, however, the spatial velocity in a rigid zone has three unknown components and their determination necessities the setting up of three equations from the mass continuity condition. Thus the spatial elementary rigid region for a three deformation problem must be tetrahedral in shape. This is the basis of the SERR technique as proposed by Gatto and Giarda [5]. The above authors analyzed the extrusion of square section through wedge shaped dies with the help of the SEER technique. They also suggested method by which complex geometrical shapes like prism and pyramid can be discretized into elementary tetrahedrons. As illustrated in subsequent chapter the above method is suitable for the upper bound analysis of section involving re-entrant corners. The limitation of this technique appears to be applied only when the deformation zone is bounded by planner faces.

The SERR is based upon discretizing the deformation zone into basic tetrahedral rigid blocks, with each block being separated from the others by planes of velocity discontinuity. Each rigid block has its own internal velocity vector consistent with the bounding conditions.Thus, if there are N rigid blocks, then the number of unknown internal velocity vectors are also N (thus, 3*N spatial velocity components).* The velocity at entry to the deformation zone (the billet velocity) is considered to be prescribed and the velocity at the exit has a single component, since its direction is known from the physical description of the problem. The total number of unknown velocity components can be uniquely determined if an equal number of equation so generated become consistent and determinate if and only if the SERR blocks are tetrahedral in shape, so that the number of triangular bounding faces automatically becomes 3N+1. To illustrate the application of the above principles, let the i_{th} bounding face in the assembly of tetrahedrons be:

$$\Phi = f(x,y,z) = a_{1i}x+a_{2i}y+a_{3i}z+1=0 \quad \ldots\ldots\ldots\ldots\ldots\ldots\ldots\ldots \quad (2.6)$$

The coefficients a_{1i}, a_{2i} and a_{3i} in above eqn. can be determined by specifying the co-ordinates of the three vertices of this triangular face. Then the unit normal vector to this face is given by the relation.

$$\hat{n} = \nabla \phi \; / \left| \nabla \phi \right| \quad \ldots\ldots\ldots\ldots \quad (2.7)$$

2.3 Discretization of Deformation zone in Extrusion

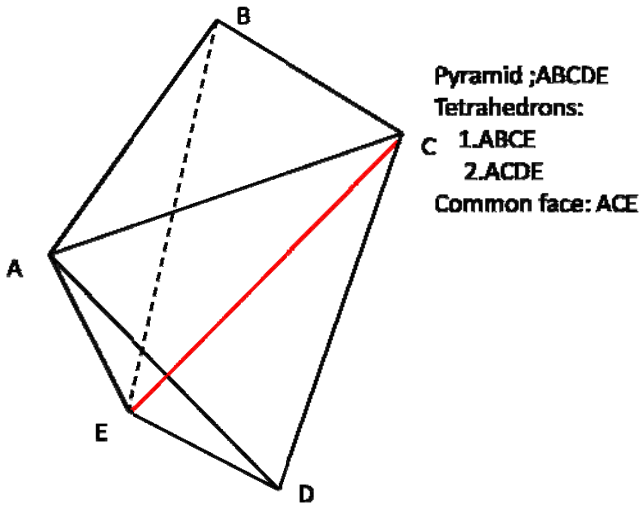

Fig. 2.3 Discretization of a pyramid into Tetrahedrons

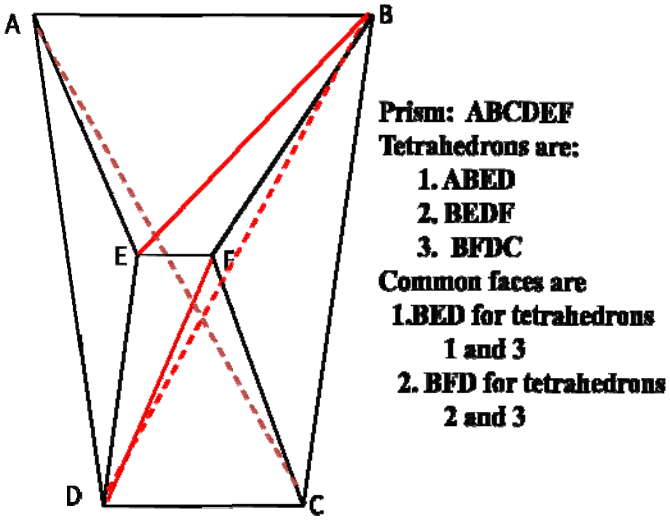

Fig 2.4 Discretization of prism in to three tetrahedrons

The deformation zone in extrusion may consist of simply a pyramid as in case of extrusion of triangular section during taking one floating point or combination of pyramids and prisms as in case of triangular section extrusion during taking double floating point. A pyramid can be discretized into two tetrahedrons as demonstrated in Fig2.3.These two tetrahedral regions have two internal velocity vectors one for each region having six components and the exit velocity can be represented by a single component by choosing a coordinate frame. When the

inlet velocity for this pyramidal zone is prescribed, there are seven unknown velocity components to be determined to establish the velocity field. Thus seven equations are necessary and sufficient to determine the velocity field. The two tetrahedrons of pyramidal region have a common face. Thus there are seven independent bounding faces which on applying the continuity condition, generate a set of seven equations which contain the unknown velocity components on solving this set of seven velocity equations, the velocity field is uniquely determined. In similar fashion, a prism can be discretized into three tetrahedrons with ten independent bounding faces that can generate a set of ten velocity equation for establishing the corresponding velocity field. The discretization of a prism into tetrahedrons shown in Fig2.4. When a deformation zone consists of a combination of pyramid and prisms the discretization of the combined region into tetrahedrons and subsequently application of continuity condition to all the independent bounding faces, generate a system of determinate velocity components. The prism and pyramid can be discretized into 3 tetrahedron and 2 tetrahedron in 6 and 2 different ways respectively shown in table 2.1.

TABLE 2.1 Conversions of Prism and Pyramid into Tetrahedron

Structure	Total No. of Tetrahedrons	No. of Ways
Pyramid	2	2
Prism	3	6

2.4 The Continuity of a Discontinuous Velocity Field

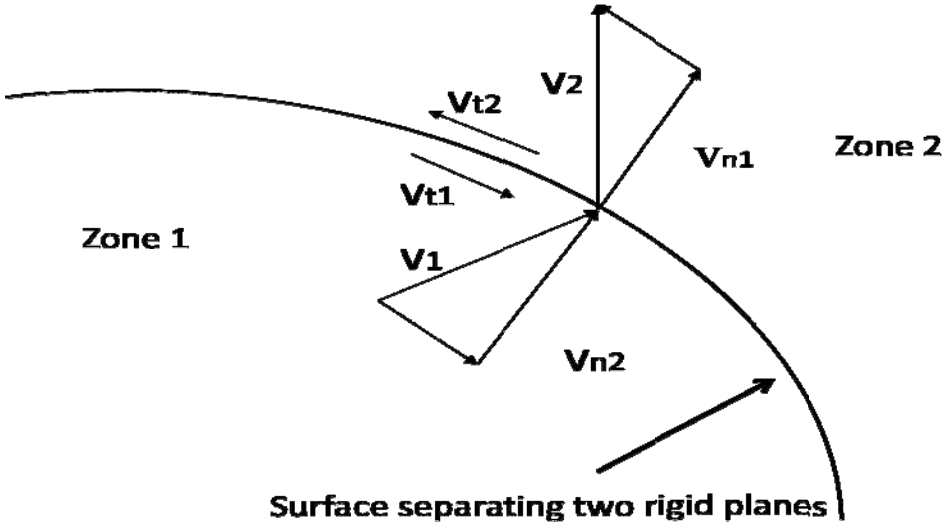

Fig 2.5 A general surface separating two rigid region

The Fig 2.5 Shows a surface separating two spatial region with v_1 and v_2 as the velocity vector on both sides. The components of these two vectors normal to the separating surface ϕ are given by the equation (2.8) and (2.9)

$$\vec{V}_{1n} = \hat{n}.\vec{V}_1 = (\nabla\phi / |\nabla\phi|).\vec{V}_1 \quad \ldots\ldots\ldots\ldots\ldots\ldots \quad (2.8)$$

$$\vec{V}_{2n} = \hat{n}.\vec{V}_2 = (\nabla\phi / |\nabla\phi|).\vec{V}_2 \quad \ldots\ldots\ldots\ldots\ldots\ldots.. \quad (2.9)$$

If A and ρ denotes the surface area of the segment and the material density respectively, then the mass flow rate across the surface segment taken from both sides. Thus the mass continuity condition (also known as volume constancy condition, since the material is incompressible) i.e.

$$(\rho A)_1.V_{1n} = (\rho A)_2.V_{2n} \quad \ldots\ldots\ldots\ldots\ldots\ldots \quad (2.10)$$

From above equation canceling $|\nabla\phi|$ which is scalar quantity so that V_{1n} and V_{2n} must equal, so;

$$\nabla \phi . \vec{V}_1 = \nabla \phi . \vec{V}_2 \quad \ldots\ldots\ldots\ldots\ldots\ldots \quad (2.11)$$

It is to be pointed out that the regions on both sides of the surface ϕ in Fig (2.5) are rigid if $\vec{V}_1$ and $\vec{V}_2$ are constant velocity vectors if equation (2.10) is linear. The linearity of equation (2.10) is assured when the surface ϕ is a plane. Thus the bounding faces of the spatial elementary rigid region can only be planner. Some of this bounding face may lie on the die surfaces or planes of symmetry. Since no material flow occurs across faces. Equation (2.10) takes the following form;

$$\nabla \phi . \vec{V}_1 = 0 \quad \ldots\ldots\ldots\ldots\ldots\ldots\ldots\ldots\ldots\ldots \quad (2.12)$$

The equation of each of the triangular faces can be determined when the co-ordinates of three vertices are specified. Then the velocity equation can be formed by applying the mass continuity condition either in the form of equation (2.10) or (2.11) as appropriate. The velocities of material in the zones are V_1 and V_2 respectively are not identical. The components of velocity in the normal and tangential direction of the surface are V_{n1}, V_{n2} and V_{t1},V_{t2}. The normal velocity V_{n1} should be equal to V_{n2} for the continuity of the material. The tangential velocity V_{t1} and V_{t2} need not be equal. The difference is called the velocity discontinuity ΔV and is given by equation (2.13).

$$\Delta V = V_{t1} - V_{t2} \quad \ldots\ldots\ldots\ldots\ldots\ldots\ldots\ldots \quad (2.13)$$

2.5 Solution to Plain Strain Problem

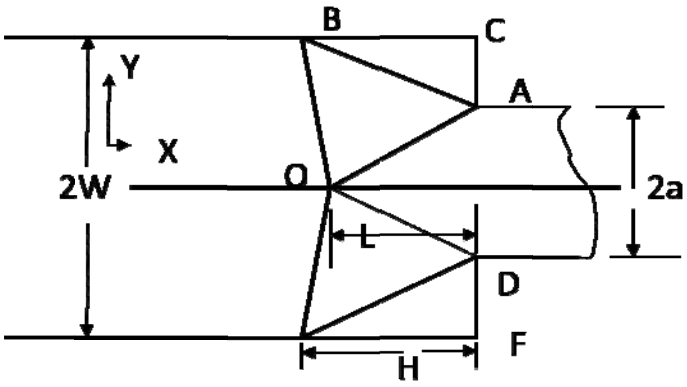

Fig 2.6 Solution of a Plain Strain Extrusion

The method of solution elucidated in the previous section is illustrated here taking the example of a plan strain extrusion process. The geometry of the process is shown fig2.6 for a through square die. Dead metal Zones ABC and DEF are formed on both side of the extrusion axis. Only one half of the deformation zone, consisting of the triangle ABO, is considered for this analysis. Thus, this triangle planner elementary rigid region is bounded by lines AB, BO and AO which are also lines of velocity discontinuity. The co-ordinate frame Shown fig2.6 is taken such that the x-axis coincides with the extrusion axis. Therefore the billet and product velocity vectors have only one component each. The co-ordinates of the vertices A, B and O are (o, a), (-H, W) and (-L, o) respectively. It is to be noted here that while a and W are known parameters, being the half widths of the product and the billet respectively, L and H are two parameters of the deformation zone which are not a prior known. H is the overall length of the deformation zone along the extrusion axis and L is the distance of the flow of the floating floating-O from the midpoint of the die orifice. These two lengths are to be selected such that the power of deformation becomes minimum. Mathematically speaking, L and H are the variable with respect to the deformation power is minimized.

In terms of the co-ordinates of the vertices, the equations of the three bounding lines are given by

$$\text{Line AB} : [((W-a)/H).\, x] + [y-a] = 0 \ldots\ldots\ldots\ldots \quad (2.14)$$

$$\text{Line BO}: [(W / (H-L)).x] + y + W.L/ (H-L) = 0 \ldots\ldots \quad (2.15)$$

$$\text{Line OA} = ((a/l).x) + y - a = 0 \ldots\ldots\ldots\ldots \quad (2.17)$$

If the billet velocity Vb is prescribed, there are three unknown velocity component in this case. These components are Vp, the product velocity, and Vx and Vy, the x- and y-components of the velocity vector in the elementary rigid region.

The line AB in fig2.6 is the limiting line for the dead metal zone. Material enters the deformation zone across line BO and the product leaves the deformation zone through line AB. Table2.2 shows these lines and the corresponding velocity vectors on both side of the line. The physical description of side of each line is also known this table.

Employing the mass continuity condition given equation (2.11) and (2.12) as appropriate to these lines, the three velocity equations are obtained as given below:

$$[(W-a) / H]. Vx + Vy = 0 \quad (2.18)$$

$$[W /(H-L)] . Vx + Vy = [W / (H-L)] . Vb \quad (2.19)$$

TABLE 2.2

Lines. The zone they separated and velocity vector on their sides.

Lines and their equations	Side 1	Velocity vector on side 1	Side 1	Velocity vector on side 1
AB $\varphi=[(w-a).x]/L+[y-a]=o$	Deformation zone	$_iV_x + _jV_y$	Dead metal zone	0
BO $\varphi=Wx/(H-L)+y+WL/(H-L)=0$	Deformation zone	$_iV_x + _jV_y$	Billet	iVb
OA $\varphi=[ax/L]+y-a=0$	Deformation zone	$_iV_x + _jV_y$	product	iVp

$$(-a/L) . Vx + Vy = - (a/L)\ 0.\ V_p \ldots\ldots\ldots\ldots \quad (2.20)$$

On solving this set of linear equation V_x, Vy and Vp, the velocity vectors are obtained as shown in equations (2.21) (2.22) (2.23).

$$V_x = (H.\ w.\ Vb) / (H.a + L.W - a.L) \ldots\ldots\ldots\ldots\ldots\ldots . \quad (2.21)$$

$$V_y = [(W-a)\ W.\ V_b)\ ] / [\ H.a = L.W-a.L\ )\ldots\ldots\ldots\ldots\ldots \quad (2.22)$$

$$V_{p=} W\ Vb / a \ldots\ldots\ldots\ldots\ldots\ldots\ldots\ldots\ldots\ldots\ldots\ldots\ldots\ldots\ldots\ldots \quad (2.23)$$

Since the elementary region is rigid, the strain rate tensor in region is zero. Therefore the power for internal deformation, J_1 is zero. Further, the dead metal zone separates the deformation zone from the die surface and as such, there is no relative motion between the two. Therefore there is no dissipation power due to the friction at the diameter faces i.e. J_3=0). Thus the power consumed for deformation is dissipated only at the lines of velocity discontinuity. Therefore in this case, equation (2.1) reduces to the following form.

$$J=J_1\ldots\ldots\ldots\ldots\ldots \quad (2.24)$$

In the present analysis, all the lines of velocity discontinuity separate rigid regions. Hence the absolute values of the velocity discontinuities at each line are constant. If $S_{AB}, S_{BO} and S_{OA}$ denote the length of the line segment AB, BO and OA respectively and, $|\Delta V|_{BO}$,and $|\Delta V|_{OA}$ represents the corresponding absolute values of the velocity discontinuities, the value of J becomes as

$$J=\left(\sigma_0 / \sqrt{3}\right)\left[|\Delta V|_{AB} + S_{AB} + |\Delta V|_{BO}\ S_{BO} + |\Delta V|_{OA}\ S_{OA}\right] \quad \ldots\ldots\ldots\ldots\ldots \quad (2.25)$$

The upper bound to the deforming power can be calculated using equation. (2.25) the upper bound so obtained can be optimized with respect to the parameter H and L and the minimum upper bound, Jmin, to the deformation power can be obtained corresponding to this velocity field. The average extrusion pressure, non-dimensional zed by σ_o, c then can be calculated form the equation.

$$P_{avg} / \sigma_0 = J_{mm} / WV_b\sigma_o \quad \ldots\ldots\ldots\ldots\ldots\ldots\ldots\ldots\ldots \quad (2.26)$$

CHPTER THREE

UPPER BOUND ANALYSIS FOR EXTRUSION OF 'TRIANGULAR' SECTION THROUGH TAPER DIES

CHAPTER 3

UPPER BOUND ANALYSIS FOR EXTRUSION OF TRIANGULAR SECTION THROUGH TAPER DIES

3.1 Introduction

Triangular section bars are produced by extrusion using taper dies. Softer metal like lead aluminum are easily extruded such sections are widely used for commercially and house hold items because their decorative value. Extrusion is carried out with the help of taper dies. For extrusion of sections taper dies with lubricant is more preferred as it provides gradual change in shape and reduction of area simultaneously.

However upper bound solution for extrusion of triangular section from round billet using taper wall with re-entrant corner received the attention of many investigators. The SERR technique is further modified for analyzing the extrusion process from round billets. In present work the circular section of round billet is approximated to 12 sides of regular polygon.

Here number of sides of polygon is increased continuously up to the limit when after increasing the sides there will be no effect on result of extrusion pressure. Here to approximate a circular section into regular polygon, sectional area must be maintained constant as shown in Fig.3.1 and by using formula given in equation (3.1).

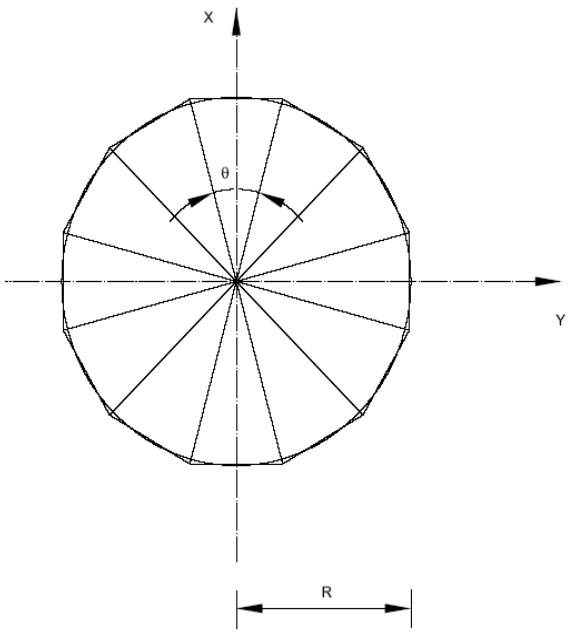

Fig 3.1 Approximation of a circular section into regular polygon of side (12)

$$\pi R^2 = \frac{1}{4} M L^2 \cot(\theta / 2) \quad \text{.....} \qquad (3.1)$$

From considerations of symmetry, only one half of the deformation zone is considered for this analysis. Where R= Radius of the round billet

M=No. of polygon sides

L=Die length

θ=Equivalent cone angle

The upper bound load has been computed using discontinuous velocity field. The discontinuous velocity field has been obtained by discritizing the deformation zone into tetrahedral blocks using reformulated SERR technique.

3.2 SERR Method Analysis

As discussed in the previous chapter, it was pointed out that in the SERR method of analysis, the deformation zone is discritized into rigid region thus leading to a discontinuous velocity field. When these rigid region are in shape of tetrahedron a determinate set of equation is obtained (by application of continuity condition to individual

faces defining the rigid region) from which the velocity component in such rigid region can be calculated. In present analysis it is assumed the centre of gravity of die aperture lies on billet axis. This assumption is necessary so that product remains straight as it is comes out of the die orifice. It is appropriate to mention that friction surface zone are part of purposed velocity field (zone of zero velocity) and upper bound theorem admits any velocity field as long as it is kinamatically admissible. For one half of the deformation geometry for triangular section because symmetry about one plane. The sub zones of deformation are delineated in domain of interest by taking suitable located floating points. For triangular section two floating point formulation gives the more upper bound solution as compared to single floating point formulation. The Fig 3.2 shows the one half of the deformation zone of 12 sides for analysis.

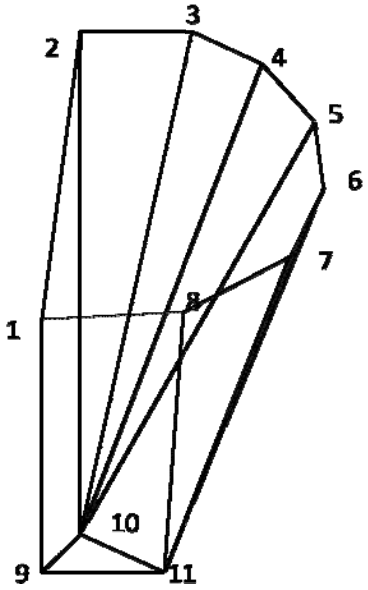

Fig 3.2 One half of the deformation zone of 12 sided polygon

3.3 Single floating point formulation

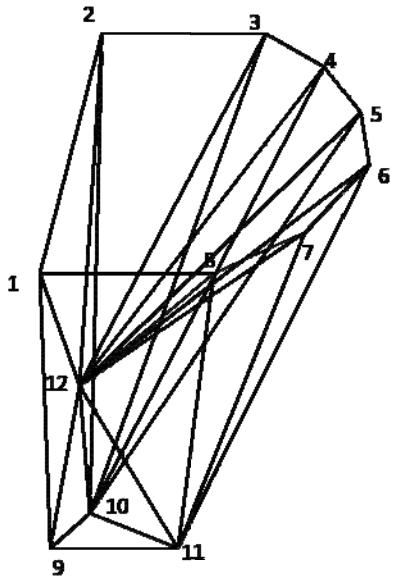

Fig.3.3 Single point formulation

In Fig.3.3 analysis is done by taking one floating for the as domain interest for discretizatio. The deformation zone is to be descritized into two pyramidal subzones (12–5–6–11–10 and 12–8–7–9–11) & five tetrahedral subzones (11–12–10–2, 3–12–10–4, 4–12–10–5, 6–12–11–7and 7–12–11–8).Hence it results in nine tetrahedrons and the number of global schemes of discritizing of different zones.

3.4 Double floating point formulation

As mentioned earlier the Traingular-sections have symmetry about one axes and therefore only one half of the extrusion geometry may be considered as domain of interest for this analysis. As it is discussed earlier that, if we increase the sides of the regular polygon of round cross section of billet, the upper bound solution falls towards the minimum value and at last it converges to give a constant result.

Hence for simplicity in explaining the double point formulation, a 12 sided regular polygon is being taken for the consideration, Fig3.4 shows the one half of the die cavity with pertinent co-ordinate system.

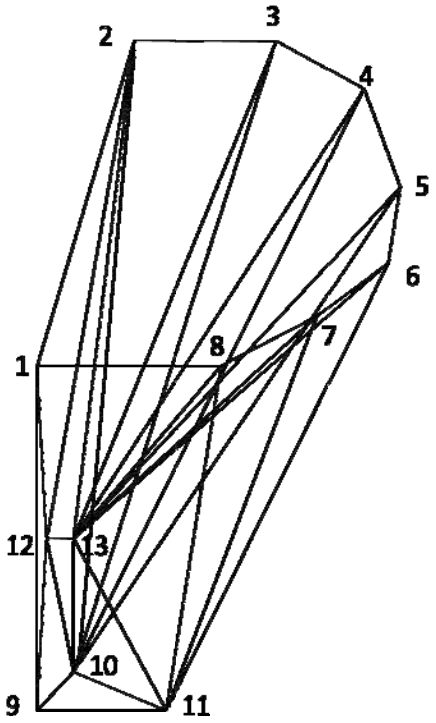

Fig.3.4 Double point formulation

In this, formulation floating point (12) is taken along symmetry plane and another floating point (13) is taken any where inside deformation zone as shown in above Fig 3.4. The deformation zone is delineated by joining corner points of entry and exist plane to the points known as floating points. By this process the deformation zone is divided into seven sub-zones, one prism, two pyramids and four tetrahedrons shown in Fig 3.5 and shown in Table 3.1 for classifying the different planes.

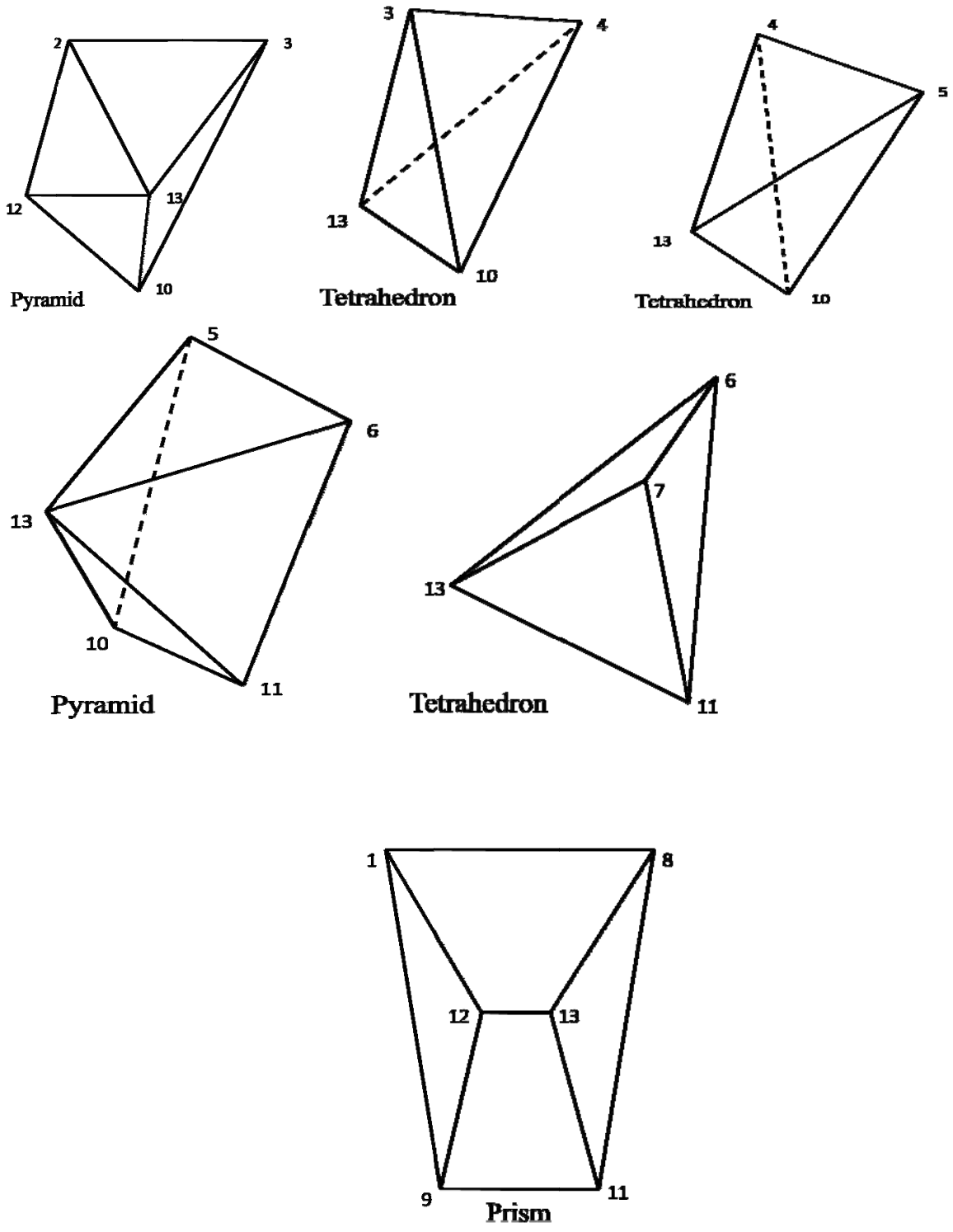

Fig 3.5 different shape of deformation zone

TABLE 3.1

Half extrusion zone (domain of interest) divided into prism, pyramid and tetrahedron

Sub-zones	Model numbering system	No. of plane faces
1.Prism	1-8-9-11-12-13	10
2.Pyramid	2-3-10-12-13	7
3.Pyramid	5-6-10-11-13	7
4.Tetrahedron	3-4-10-13	4
5.Tetrahedron	4-5-10-13	4
6.Tetrahedron	6-7-11-13	4
7. Tetrahedron	7-8-13-11	4

.

Each prism can be subdivided into three tetrahedron in six different ways and each pyramid can be divided into two tetrahedron in two different ways as discussed earlier. Hence the total deformation zone can be subdivided into 11 numbers of tetrahedrons in 24 different ways i.e. (2×2×6) shown in Table 3.2 and total number of plane derived from the prism, pyramid and tetrahedron shown in Table 3.3 .

TABLE3.2

Number of planes and ways of discritization

No. of Tetrahedrons	No. of Planes	No. of Ways
1×3+2×2+1+1+1+1=11	11×4-10(common plane)=34	6×2×2

TABLE 3.3

Total number of planes derived from Prism, Pyramid and Tetrahedrons;

Subzones	Model numbering system	Numbering of different planes	No. of planes	Total no.of common planes	Total no. of planes
Prism	1-8-9-11-12-13	1-12-9 1-9-8 1-9-11 1-8-12 1-8-11 8-9-12 8-11-13 8-9-11 8-9-13 9-11-13	10	7-13-11 4-10-13 8-13-11 3-10-13 5-10-13 6-11-13 (6 Common planes)	(10+7+7+4+4+4+4) - 6 =34
Pyramid	2-3-10-12-13	2-3-13 3-10-13 10-12-13 2-12-13 3-12-13 2-12-13 3-10-12	7		
Pyramid	5-6-10-11-13	5-6-13 6-10-13 6-11-13 10-11-13 5-13-10 5-6-10 6-10-11	7		
Tetrahedron	3-4-10-13	3-4-10 3-4-13 3-10-13 4-10-13	4		
Tetrahedron	4-5-10-13	4-5-13 4-5-10 4-10-13 5-10-13	4		
Tetrahedron	6-7-11-13	6-7-11 6-7-13 6-11-13 7-11-13	4		
Tetrahedron	7-8-13-11	7-8-11 7-8-13 7-13-11 8-11-13	4		

3.5 Calculation of velocity components

Each tetrahedron move with a unique velocity. The internal velocity of each tetrahedron is V_1, V_2, and V_3 …….. V_{11} (as there are 11 numbers of tetrahedrons) when resolved into components along the co-ordinate axis V_1, V_2, V_3 …….. V_{11} together have 33. The billet and product velocity vector, Vb, Ve are along the extrusion axis (z-axis) and so can be consider to have one non-zero component each. With prescribed billet velocity Vb, the product velocity Ve is taken as unknown thus there are 34 unknown velocity components. When mass continuity condition is applied to all 34 bounding faces of these 11 tetrahedrons, then 34 equations are obtained. These 34 equations being a determinate set are solved simultaneously to give the all unknown velocity components.

Here the floating point (12) has 2 unknown co-ordinate whereas (13) has 3 unknown co-ordinates. Using these co-ordinates, the equation of plane containing 34 triangular faces under consideration can be determined. Since a velocity discontinuity is permissible only along the tangential direction the normal component on side of faces must be equal. A validity of equation carried out under following consideration (velocity on both side of each face is given in table3.5)

(a)Normal velocity in friction surface is zero.

(b) Normal velocity in symmetry plane is same.

With this theoretical approach a matrices of (34×35) with suitable sub-program is solved to get required unknown velocity component (V_{1x}, V_{1y}, V_{1z}) ……(V_{11x} ,V_{11y}, V_{11z})and V_e along Z-direction . After getting the velocity components, the resultant velocity at each plane faces are then carried out.

$$V_1=\sqrt{\ }[V_1x^2+V_1y^2+V_1z^2] \quad (3.2)$$

$$V_2=\sqrt{\ }[V_2x^2+V_2y^2+V_2z^2] \quad (3.3)$$

$$V_{11}=\sqrt{}\,[V_{11}x^2+V_{11}y^2+V_{11}z^2] \qquad (3.4)$$

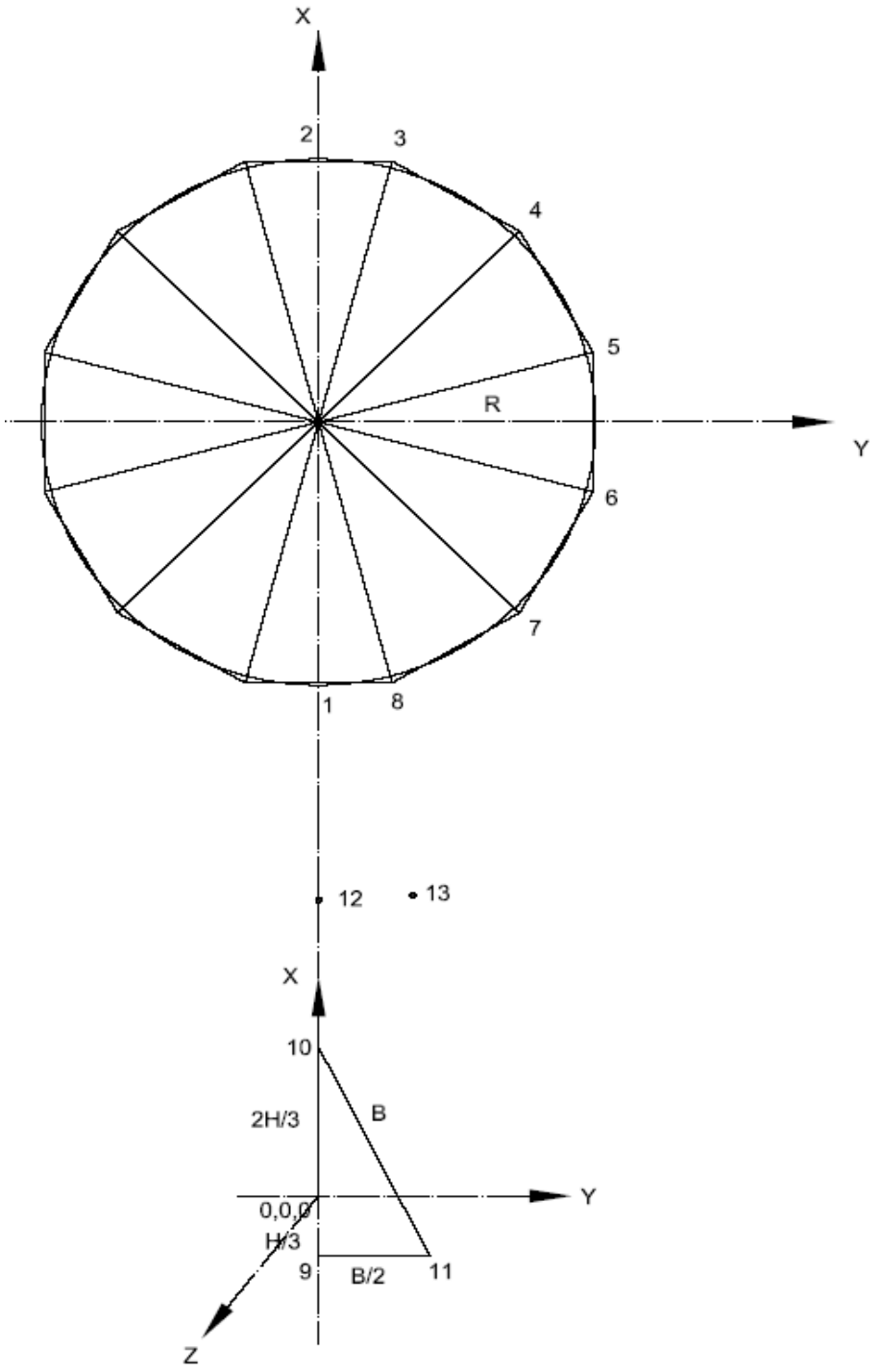

Fig 3.6 Co-ordinate of the half of the TRIANGULAR section

TABLE3.4

Co-ordinates of points in deformation zone

Points	X-co-ordinate	Y-co-ordinate	Z-co-ordinate
1	-R	0	L
2	R	0	L
3	R Cos(π/12)	R Sin(π/12)	L
4	R Cos(π/4)	R Sin(π/4)	L
5	R Cos(5π/12)	R Sin(5π/12)	L
6	R Cos(7π/12)	R Sin(7π/12)	L
7	R Cos(9π/12)	R Sin(9π/12)	L
8	R Cos(11π/12)	R Sin(11π/12)	L
9	-H/3	0	0
10	-2H/3	0	0
11	-H/3	B/2	0
12	0	Y_{12}	Z_{12}
13	X_{13}	Y_{13}	Z_{13}

Knowing the co-ordinates of point's equation of all triangular faces (34) can be found out. But for simplicity a mathematical approach for equation of triangular face 4-5-10 can be express as matrices of (4×4)

$$\begin{vmatrix} \mathbf{X} & \mathbf{Y} & \mathbf{Z} & \mathbf{1} \\ \mathbf{R\,Cos(\pi/4)} & \mathbf{R\,Sin(\pi/4)} & \mathbf{L} & \mathbf{1} \\ \mathbf{R\,Cos(5\pi/12)} & \mathbf{R\,Sin(5\pi/12)} & \mathbf{L} & \mathbf{1} \\ \mathbf{-2H/3} & \mathbf{0} & \mathbf{0} & \mathbf{1} \end{vmatrix}$$

Similarly equation for all 34 planes can be set up. With this theoretical approach a matrices of (34×35) with suitable sub-program is solved to get required unknown velocity components i.e. (V_{1x},$V_{1x,}$ V_{1z})(V_{2x}, V_{2y}, V_2z)…… (V_{11}x,V_{11y},V_{11z}) and V_e along Z-direction. After getting the velocity components, the resultant velocity at each plane is then carried out.

3.6 Calculation of area of triangular faces in deformation zone

Knowing the co-ordinates of each plane face in deformation zone then area of triangle is calculated. Co-ordinate of these vertices of triangle in the space are ($X_{1,}Y_{1,}Z_1$), ($X_{2,}Y_{2,}Z_2$) ($X_{3,}Y_{3,}Z_3$)

Area of triangle is

$$A = \sqrt{(A_X)^2 + A_y^2 + A^2{}_z} \quad \text{……..} \qquad (3.5)$$

$$A_x = \tfrac{1}{2}\left(y_1z_2 - y_2z_1 + y_2z_3 - y_3z_2 + y_1z_3\right) \quad \text{……..} \qquad (3.6)$$

$$A_y = \tfrac{1}{2}\left(x_1z_2 - x_2z_1 + x_2z_3 - x_3z_2 + x_1z_3\right) \quad \text{…….} \qquad (3.7)$$

$$A_z = \tfrac{1}{2}\left(x_1y_2 - x_2y_1 + x_2y_3 - x_3y_2 + x_2y_3\right) \quad \text{…….} \qquad (3.8)$$

Using the above equation the area of the bounding faces is calculated,

$$A_n = (A_1 + A_2 + A_3 + A_4 + A_5 + \text{……..} + A_{34}) \quad \text{……..} \qquad (3.9)$$

When A_n is total area of bounding faces and n is the number of bounding faces of triangular shape which is taken as 34 in our assumption. Table 3.5 shows the various surfaces, types and their velocities for deformation zone of Fig 3.4.

TABLE 3.5

Various surfaces, types and their velocity

Surface	Category	Normal velocity in that surface
2-3-12-13	Entry surface	Billet velocity(Vb)
2-3-13	Entry surface	Billet velocity (Vb)
5-6-13	Entry surface	Billet velocity (Vb)
6-7-13	Entry surface	Billet velocity (Vb
7-8-13	Entry surface	Billet velocity (Vb)
4-5-13	Entry surface	Billet velocity (Vb)
4-5-10	Friction surface	0
3-4-10	Friction surface	0
2-3-10	Friction surface	0
5-6-10-11	Friction surface	0
6-7-10-11	Friction surface	0
7-8-10-11	Friction surface	0
4-5-10	Friction surface	0
3-4-10	Friction surface	0
2-3-10	Friction surface	0
1-2-9-10	Symmetry surface	Equal on both sides
12-13-10-11	Exit surface	Product velocity (Vp)
12-13-9-11	Exit surface	Product velocity (Vp)
12-13-9-10	Exit surface	Product velocity (Vp)

3.7 Calculation of Non-dimensional Extrusion Pressure

Deformation power consists of power of shear deformation at the plane of velocity discontinuity and friction power at die/work piece may be determined using relation.

$$J = \sigma_0 / \sqrt{3} \sum |\nabla V_n| A_n + \sigma_0 m / \sqrt{3} \sum |\nabla V_n| A_n \ldots\ldots\ldots\ldots\ldots\ldots \quad (3.10)$$

Where n= Total no. of bounding faces

$|\nabla V_n|$ = is the velocity discontinuity at nth faces whose area is An

The non-dimensional extrusion pressure (Pav/σ_0) is optimized with respect to seven unknown adjustable or variable parameter of deformation zone and written as

$$P_{av} / \sigma_0 = J / A_b V_b \sigma_0 \ldots\ldots\ldots\ldots\ldots\ldots\ldots\ldots\ldots \quad (3.11)$$

Where A_b = Area of Billet

V_b = Billet Velocity

σ_0= Uniaxial Stress in Compression

3.8 Computation:

Using a suitable analytical model, computation is carried out. It consists of following steps:

(a) Determine the co-efficient of equation of the planes containing bounding faces of tetrahedral block.

(b) Determine the co-efficient of velocity equation by applying the mass continuity condition to respective planes.

(c) Magnitude of velocity discontinuity is found out by algorithm. This solution also determines exit velocity, with serves as check on computation. Since exit velocity can be independently calculated using billet velocity and the area reduction.

(d) Computing deformation work by equation(3.10) and non-dimensional extrusion pressure by equation(3.11)

(e) Optimizing non-dimensional extrusion pressure with respect to variable parameter L, $Y_{12}, Z_{12}, X_{13}, Y_{13}, Z_{13}$, using multivariable unconstraint routine.

(f) All the computation is carried out with a suitable subroutine of tetrahedron, pyramid, and prism imposed with different alternatives. Figs 3.7, 3.8 and 3.9 show the variation of non-dimensional extrusion pressure with equivalent cone angle at area reduction 75%, 80% and 85% for different friction factor respectively. Fig 3.10 shows the variation of non-dimensional extrusion pressure with percentage of area reduction at equivalent semi-cone angle 20˚ for different friction factor.

3.9 Optimization parameter

For a double point formulation one floating point lies on plane of symmetry having two undetermined co-ordinates Y_{12} and Z_{12}. Second floating point lies any where inside deformation zone having three undetermined co-ordinates X_{13}, Y_{13}, Z_{13}. Height of deformation zone an additional optimizing parameter.

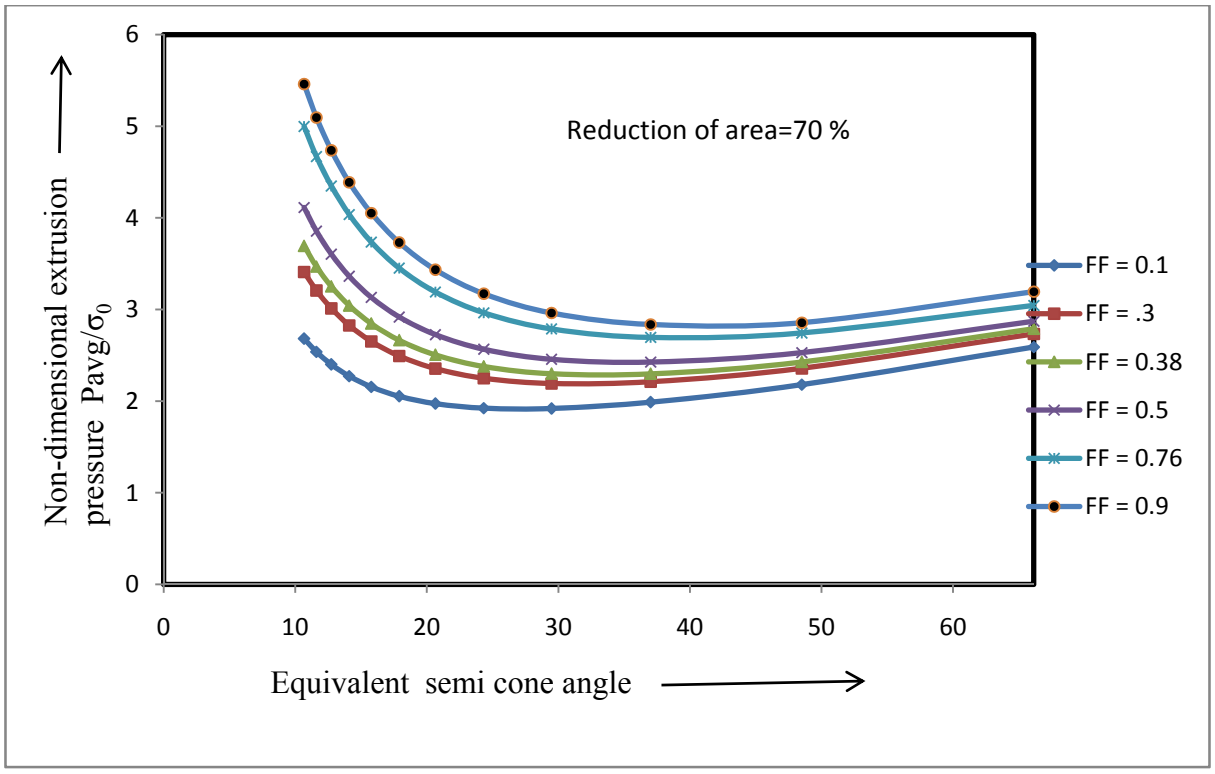

Fig.3.7 Variation of non-dimensional extrusion pressure with equivalent semi cone angle

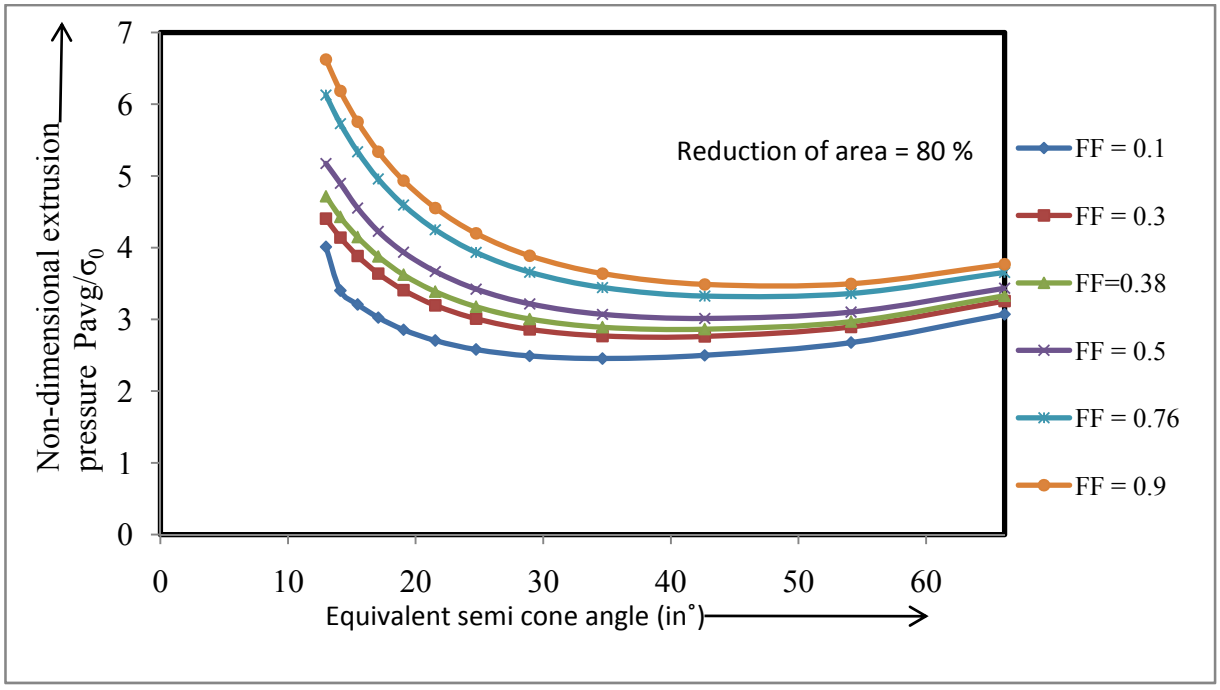

Fig.3.8 Variation of non-dimensional extrusion pressure with equivalent semi cone angle

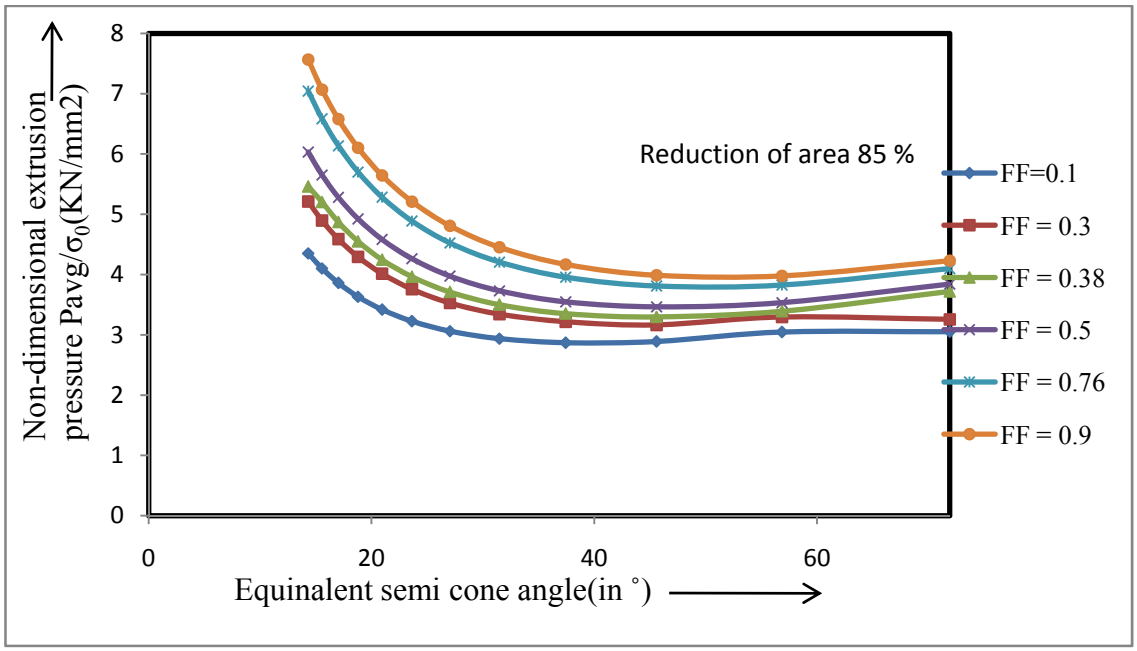

Fig.3.9 Variation of non-dimensional extrusion pressure with equivalent semi cone angle

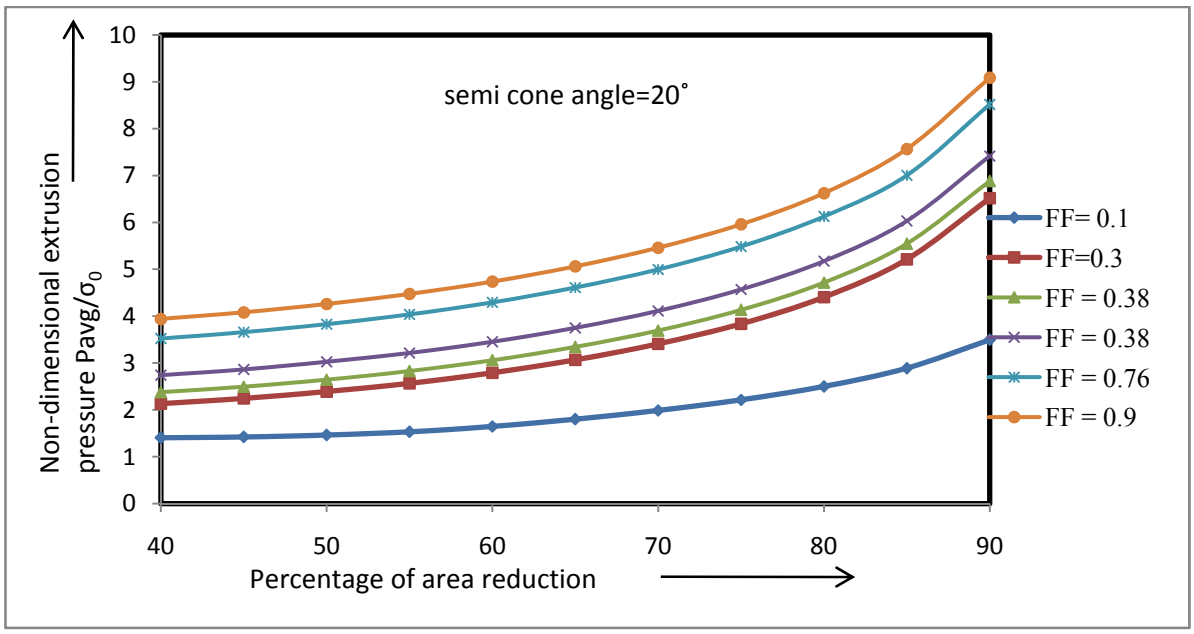

Fig.3.10 Variation of non-dimensional extrusion pressure with percentage of area reduction

3.10 Results and Discussion

Computation is carried out by approximating the round section of the billet into 12 sided regular polygons. The reformulated SERR technique is applied to find out the optimum kinematically velocity field to get the upper bound solution.

The results of computation are done for 4 schemes for single point formulation (SPF) and 24 schemes for double point formulation (DPF). It is seen that SPF gives better result than DPF, so result of SPF is taken into consideration. The scheme with least upper bound is identified and that discretization scheme is taken for finding out the non-dimensional extrusion pressure with the variation of other influencing parameters, like, reduction, friction factor and semi-equivalent cone angle. Figs 3.7, 3.8, 3. 9 show the variation of non-dimensional extrusion pressure with equivalent semi-cone angle at different reduction. From these figures it is seen that with the increase of equivalent semi cone angle the non –dimensional extrusion pressure decreases initially and then increases. This indicates there is an optimum cone angle at which the redundant work is minimum so as the extrusion pressure. Fig. 3.10 shows the increase of non-dimensional extrusion pressure with the increase of percentages of area reduction for different friction factor at 20˚ semi-cone angle. This is due to the increase of extrusion load with increase of redundant work.

CHPTER FOUR

EXPERIMENTAL INVESTIGATION

CHAPTER 4

EXPERIMENTAL INVESTIGATION

4.1 Introduction

In the upper bound analysis idealized assumptions made regarding the nature of deformation and material properties. Consequently, before applying the theoretically result to any practical situation, their adequacy needs experimental verification. The objective of present work is to compare theoretically predicted extrusion load with experimental value. Experiments are performed for TRIANGULAR section using tapper die. Commercially available tellurium lead was chosen as the working material for the experiments (extrusion). Different shape of same circular entry face and various reduction of triangular exit face were made (72.78%, 80.78%, and 87.41%).

4.2 Determination of Material Behavior

A serious limitation of the tensile test even for cold working is that fracture occurs at a moderate strain; so that it is not possible to use this test for determination of yield stress, after very heavy deformation. The fracture is most easily avoided by adopting some compressive form of test. The average stress state during testing is similar to that in much bulk deformation process, without introducing the problems of necking or material orientation.

Therefore, in compression test, a large amount of deformation can be achieved before fracture. By controlling the barreling of the specimen ends and the anvils with lubricants the strain can be varied under limits.

4.2.1 Compression Test

The simplest of these tests is the axial compression of a cylinder between smooth platens. If the platens are well lubricated, this gives essentially the same yield stress at a tensile test with small strains. As the strain is increased, the specimen spreads and thinning of the lubricant occurs, so that the frictional component at the die face increases .The increase in the load

required causing yielding. It can be overcome to a large extent by removing the sample after small increments in strain and relubricating each time. The main disadvantage of this tests is conducted at a constant true stress strain rate require special equipment. Compression testing has developed into a highly sophisticated test of workability extrusion and is a common quality control test in extrusion operation. Compression loads are applied to many engineering structures that vary in dimension from massive suspension bridge piers to the thin sheets of aircraft wings. In addition, metal forming processes involve large deformation. Analysis of metal forming processes requires knowledge of stress strain properties. The following assumptions are made in stress strain testing.

- In any test, used to obtain uniform axial compression stress strain properties, the measured quantities are generally load and strain. If a strain gage is used or displacement is measured at the surface of the specimen, the longitudinal and transverse strain is assumed to be uniform along the entire gage length.
- The cross sectional area is constant over the gage length
- The stress is uniaxial and uniform in each cross section along the gage length
- The loading forces must maintain initial alignment throughout the entire loading process
- The measured surface strain is assumed to be same as internal strain.

An error in stress or strain occurs, if the assumptions of uniformity do not exist in a test. Buckling, distributions, and elimination of these phenomena in the compression test leads to more accurate stress strain data.

To determine the uniaxial yield tress of the billet material for any given reduction, R the corresponding strain imparted to the billet material during the extrusion process must be known a prior. For the same reduction the stain imparted to the billet during the extrusion process is always higher than that imparted to the billet during compression because of redundant work done during extrusion process. Following Johnson (4) the above strain in the present case was calculated from the empirical relation.

$$\varepsilon = 0.8 + 1.5 \, Ln(1/(1-R)) \qquad \text{..... (4.1)}$$

Where R is the fractional reduction. The average yield stress of the extruded billet was then calculated by dividing the area under the stress-strain curve.

4.2.2 Experimental Procedure of compression test

Cylinders with a 50.20mm × 31.77 mm (H/D = 1.5 to 2) were used to obtain the stress-strain curve by a compression test using UTM (INSTRON 600 KN) at room temperature. The compression rate is maintained same as that adapted for the experiments. The specimen has oil grooves on both the ends to entrap lubricant during the compression test. The compression load is recorded at every 0.5 mm of punch ravel. After compressing the specimen to about 10 mm it is taken out of the press, re-machined to cylindrical shape with original diameter, and tested in compression till the specimen is reduced to about 10mm. The stress-strain diagram is drawn and the curve is extrapolated beyond a natural strain 0.5. To simulate a rigid plastic material, the wavy portion is approximated by smooth line (Fig. 4.1). The average flow stress of the used lead is found to be 25460 KN/m^2.

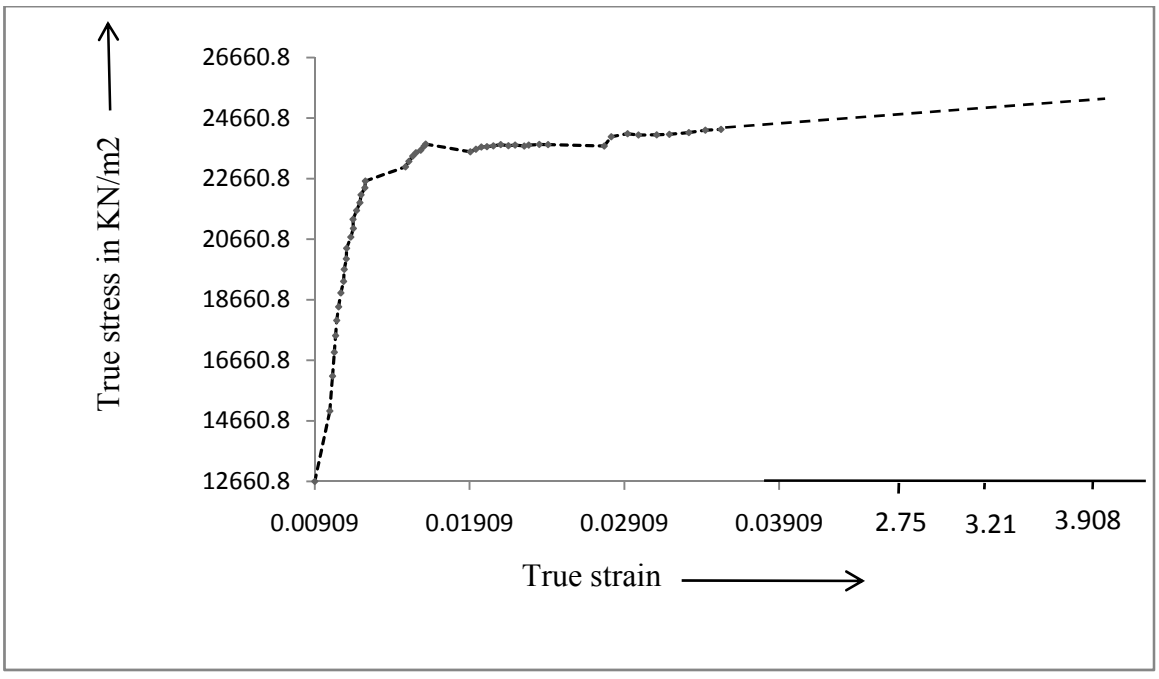

Fig 4.1 Variation of True Stress with True Strain

4.3 Measurement of Friction Factor

The local value of the friction cannot be easily determined. The coefficient of friction may actually vary through a working pass, as the lubrication deteriorates due to thinning of the film and extension of their surface. Experimental studies suggests, however that this is negligible for all well lubricated operations. There is at present no generally accepted method of measuring the value of the coefficient of friction for given surface and lubricant. Various factors can influence the result, chemical condition, lubricant film thickness; temperature, speed, environment and degree of deformation should match as closely as possible the actual conditions of the operation. The friction factor can be measured by the following methods.

- Direct measurement of friction in metal working
- Coefficients obtained from correlation of theory
- Measurements depending upon shape change.

4.3.1 Ring Compression Test

If the coefficient of friction can be deduced from a change in shape, the yield stress will not enter the derivation, provided the material is homogeneous and there are no serious temperature gradients. Such methods are generally suitable for rapidly strain hardening materials. Ring compression test suggested by Kudo and Kungio and developed by Cockcroft utilizes axial compression of a ring between flat platens. When a flat, ring shaped specimen is upset in the axial direction, the resulting shape change depends only on the amount of compression in the thickness direction and the frictional conditions at the die ring interfaces. If the interfacial friction were zero, the ring would deform in the same manner as a solid disk, with each element flowing outward radially from the center.

In case of small but finite interfacial friction, the outside diameter is smaller than in the zero friction case. If the friction exceeds a critical value, frictional resistance to outward flow becomes so high that some of the ring material flows inward to the center. Measurements of the inside diameters of compressed rings provide a particularly sensitive means of studying interfacial friction, because the inside diameter increases if the friction is low and decreases if the friction is higher. The ring thickness is usually expressed in relation to the inside and outside diameters. Under the condition of maximum friction, the largest usable specimen height is

obtained with rings of dimensions in the ratio of 6:3:1 i.e. outer diameter: inner diameter: height. For normal lubricated conditions, geometry of 6:3:2, shown in Fig 4.2, can be used to obtain results of sufficient accuracy for most applications. The ring compression test can be used to measure the flow stress under high strain practical forming conditions. Thus, by measuring the ratio of internal, external diameters after axial compression of a ring of standard dimensions, it is possible to obtain a measure of the friction.Fig.4.3 shows rings after compression.

Fig 4.2 Ring before compression

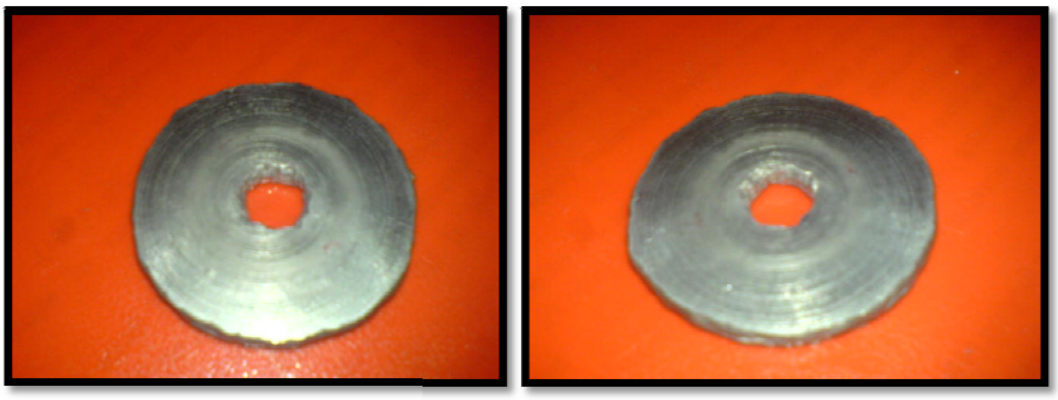

Fig 4.3Ring after compression

4.3.2 Experimental Procedure for ring test

A ring compression test was carried out at dry condition and commercially available grease lubrication condition. The rings were compressed upto the 4 mm inner diameter, at each 0.5 mm of punch travel inner diameter and height was recorded. The friction factors were found to be 0.76 for dry condition and 0.38 for the lubricated condition by comparing our result with the calibration curve of Male and Cockcroft (Fig. 4.4).

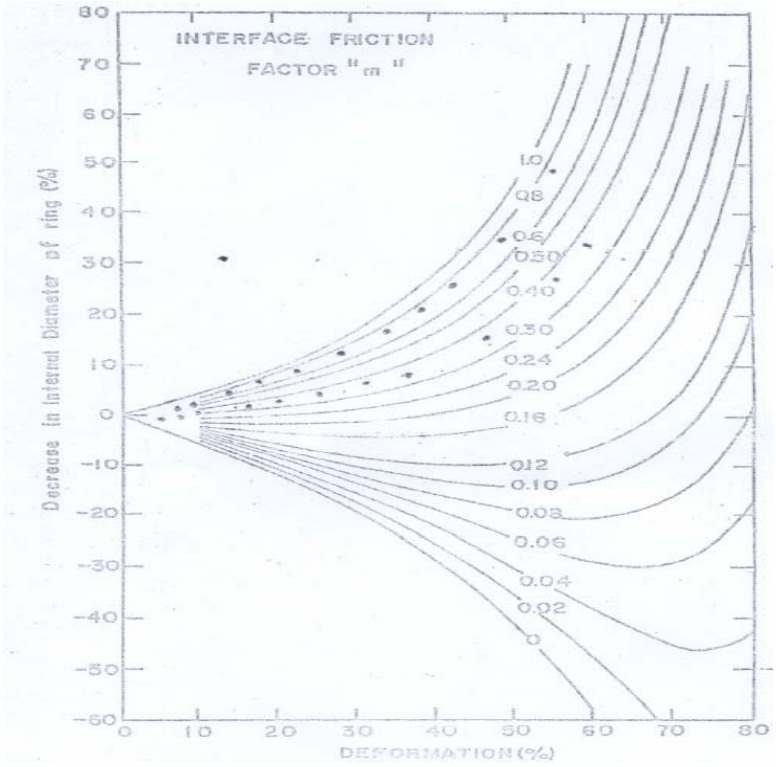

Fig 4.4 Theoretical calibration curve for standard ring 6:3:2

4.4 Experimental Setup

The following section deals with the brief description of apparatus, dies. The present studies on tapper die entry as circular and exit as a triangle. The output product is like a triangular section. The main parts namely.

(1) punch (3)die (5) base plate
(2) container (4)die hold

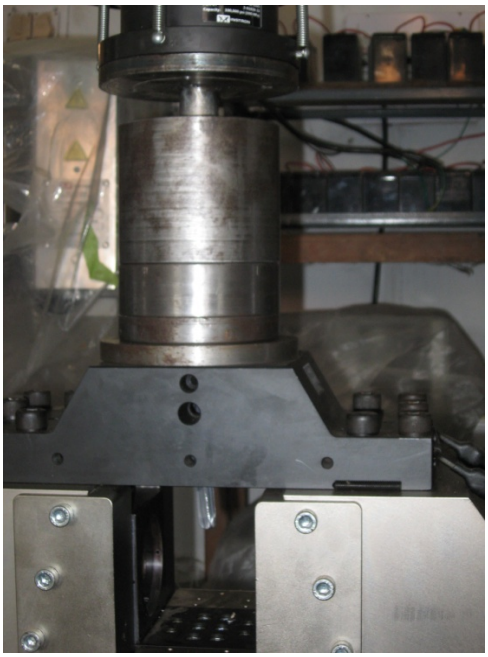

Fig 4.5UTM (INSTRON 600 KN) and UTM with close view

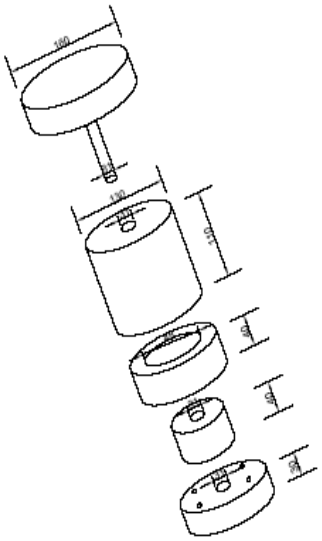

Fig 4.6Assembly setup (photo copy) Fig 4.7Shcematic view of Experimental setup

Fig 4.8 Disassemle parts of setup(photograph)

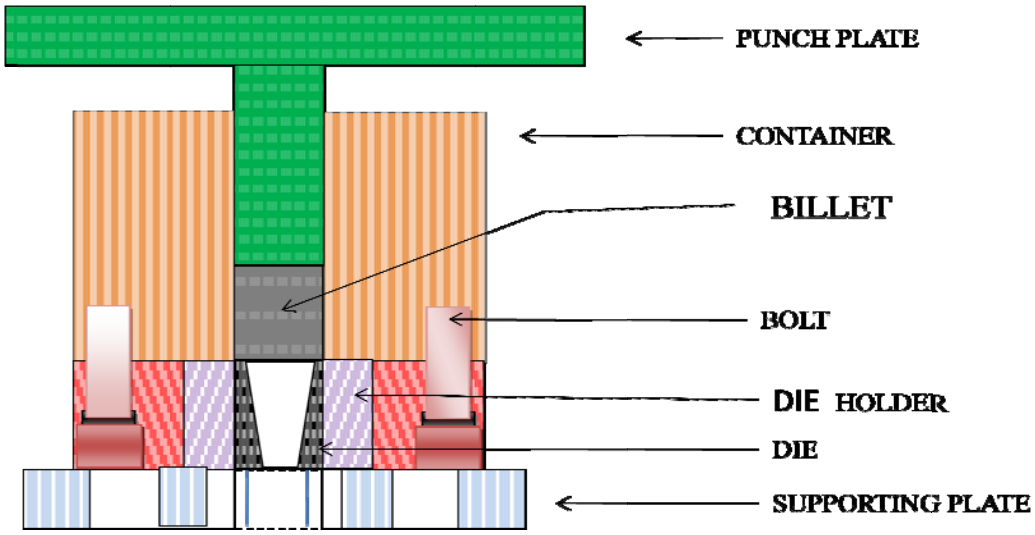

Fig4.9 Experimental setup for extrusion

Fig.4.5 shows the UTM in which the experiments were carried out. Figs 4.6, 4.7, 4.8and 4.9 are photographs of assemble parts, schematic view of parts, photograph of disassemble parts and cross sectional parts of the experimental setup respectively.

4.4.1 Different Parts of the Set-up

Container with extrusion chamber

Material: MS

Properties: tensile strength – 320 N/mm^2

Hardness - 100 BHN

Die plate

Material: MS

Properties: tensile strength – 320 N/mm^2

Hardness- 100 BHN

Punch &supporting plate

Material: MS

Properties: tensile strength – 320 N/mm^2

Hardness- 100 BHN

Die

Material: MS

Properties: tensile strength -320 N/mm^2

Hardness-100BHN

Taper dies are manufactured split type for easy removal of the product. Three dies of reductions 72.78%, 80.78% and 87.41% (Table 4.1) are made for the experiments (marked type-1 in Fig.4.10 (b)). To check the effect of orientation of inclined surface from entry to exit one number of other type (72.78% reduction), marked type-2 in Fig.4.11 (b), is made. Photograph of the dies made and used is shown in Fig 4.12. Fig 4.11(b) shows the bottom view of die which is same for both types of dies through which the triangular products are comes out.

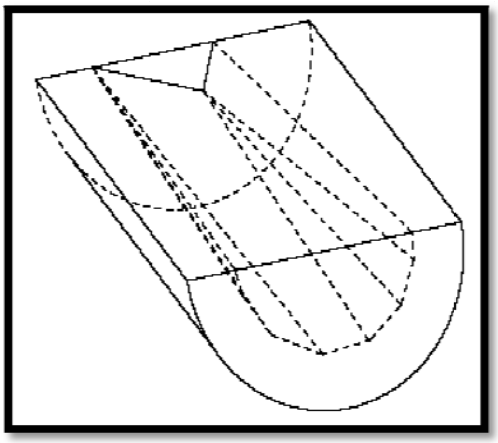

Fig 4.10 (a) One half Schematic view of die

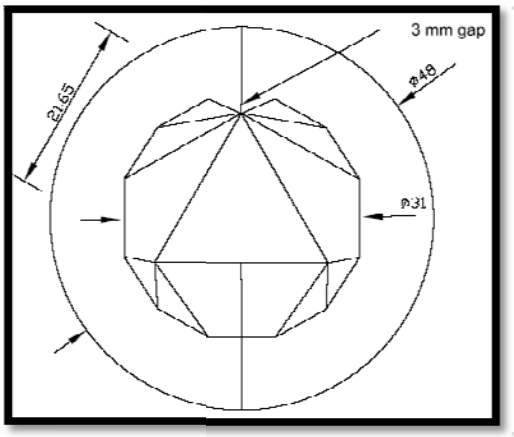

Fig4.10 (b) Top view of die TYPE 1

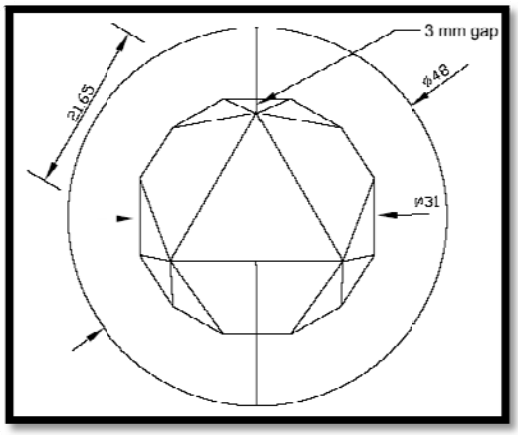

Fig4.11(a)Top view of die TYPE 2

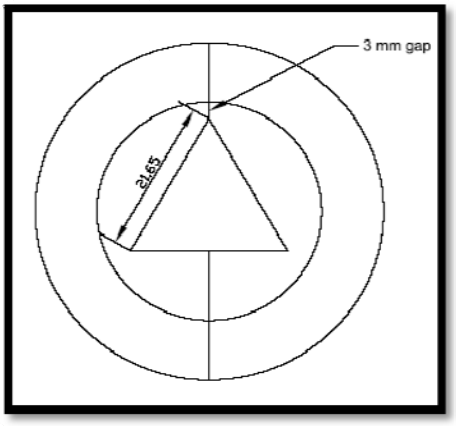

Fig4.11 (b) Bottom view of die

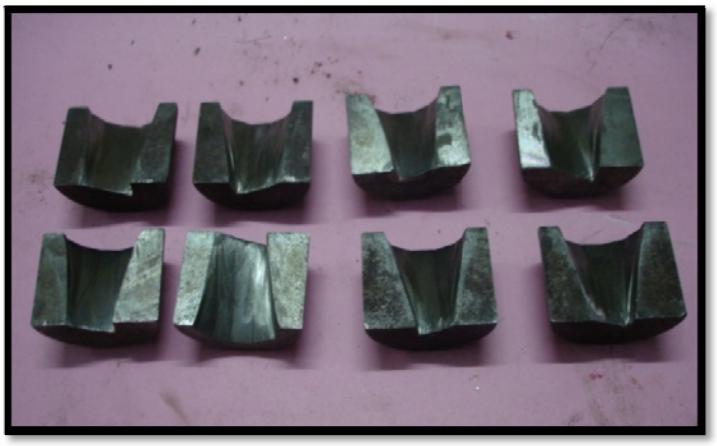

Fig 4.12 Photograph of different type of die

TABLE 4.1

Dimension of different Dies

Sl. No.	Length of side(mm)	Area (mm^2)	% of area reduction	Height of Die(mm)
1 type 1	21.65	202.97	72.78	40
2 type 1	18.18	143.32	80.78	40
3 type 1	14.72	93.85	87.41	40
4 type 2	21.65	202.97	72.78	40

Bolt

Material: harden steel

Properties: tensile strength – 390 N/mm^2

Hardness- 200 BHN

Extrude metal

Material: lead

Properties: tensile strength – 20 N/mm^2

Melting point –327 $^{\circ}$ C density -11330Kg/m^3

4.5 Experimental procedure

Before starting the test the die sets, die holder and inside face of extrusion chamber were cleaned. The two halves of the die set were then push fitted into die holder and total assembly were secured by screwing four bolts. The full assembly was then placed in the placed between the base plate of UTM (Instron 600 KN) in upside down position. It was done so that extruded product would get enough clearance, when it comes out from the die. For carrying out an extrusion test the side of lead specimen was placed in side extrusion chamber. The punch was then inserted into its position. After centering the apparatus under machine lower table, Machine was started and extrusion process was continued. The speed of movement of punch being given 1.5 mm per minute to avoid rate effect and to account for uniformity in results. Punch load was recorded at every 1.5 mm movement of punch travel, which was read from computer fitted to the UTM. The application of load was continued till it reaches the steady state and up to certain length of product comes out side. At this position Machine was stopped and test was terminated the die holder was then separated from extrusion chamber and finally die halves with extruded product were pushed out from die holder and extrusion chamber. Experiments were conducted for three different reductions (72.78%, 80.78%, and 87.41%) to get triangular section product at two different friction condition (dry-.76 friction factor, wet-.38 friction factor) from round cross-section billet. The variation of extrusion load with punch displacement is shown in Figs 4.13, 4.14, 4.15, 4.16, 4.17 and calculated results are summarized in Table 4.2. The extrapolated theoretical values at experiment conditions and comparison between experimental and theoretical results are depicted in Table 4.3. Photograph of the extruded product is shown in Figs. 4.18, 4.19 are at wet and dry condition respectively. Fig. 4.20 shows the inclined surfaces marked in the last end of the product.

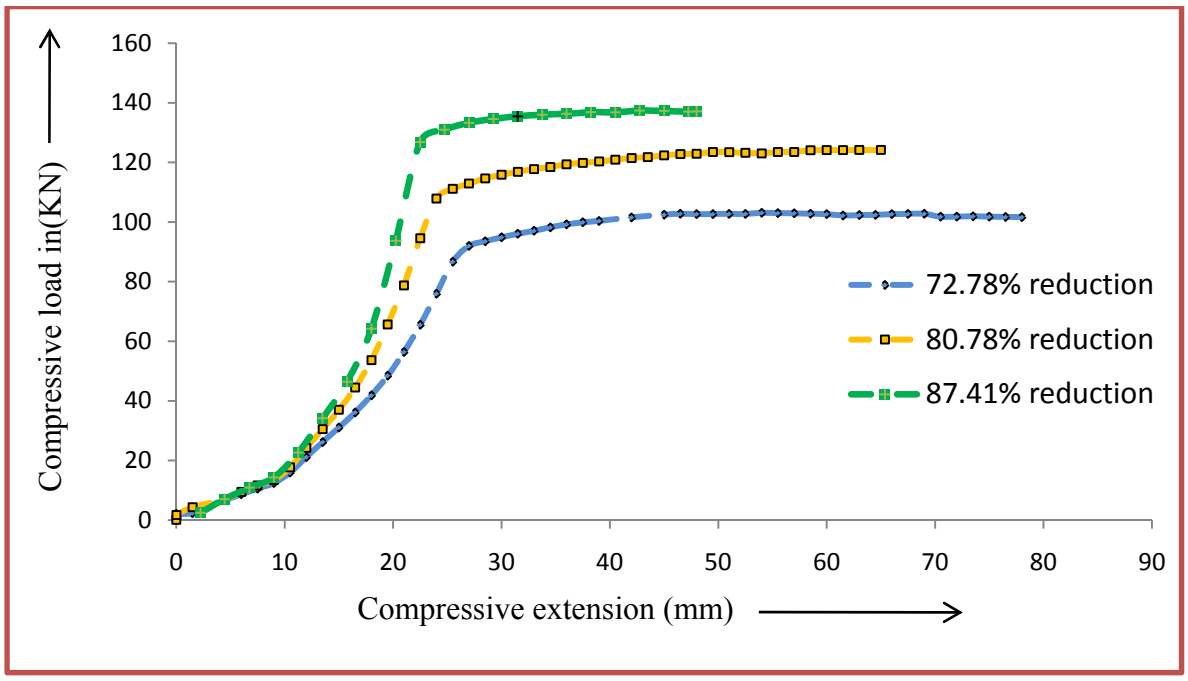

Fig 4.13 Variation of Compressive Load with Extension at Lubricated Condition

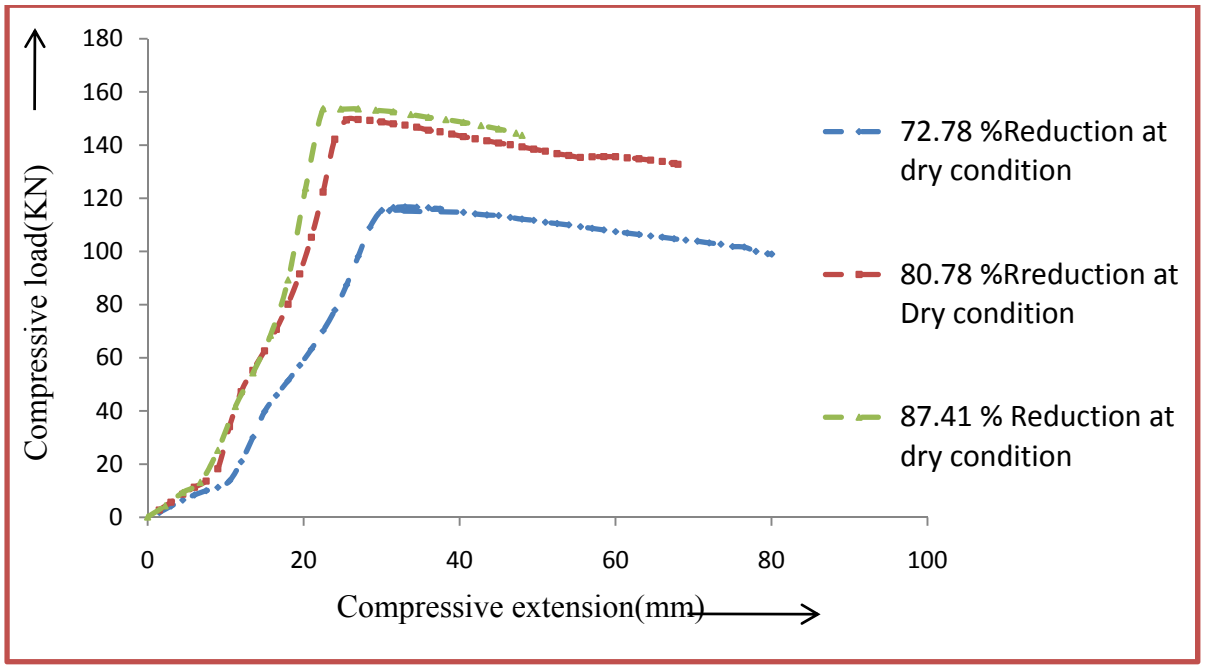

Fig 4.14Variation of Compressive Load with Extension

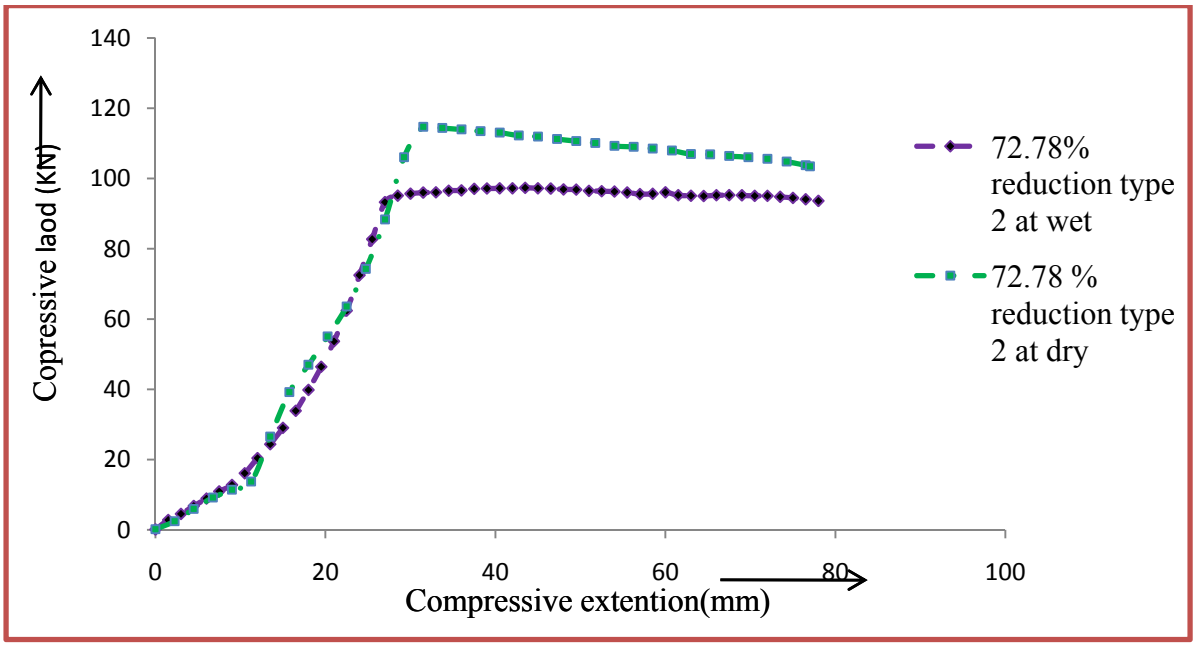

Fig 4.15 Variation of Compressive Load with Extension

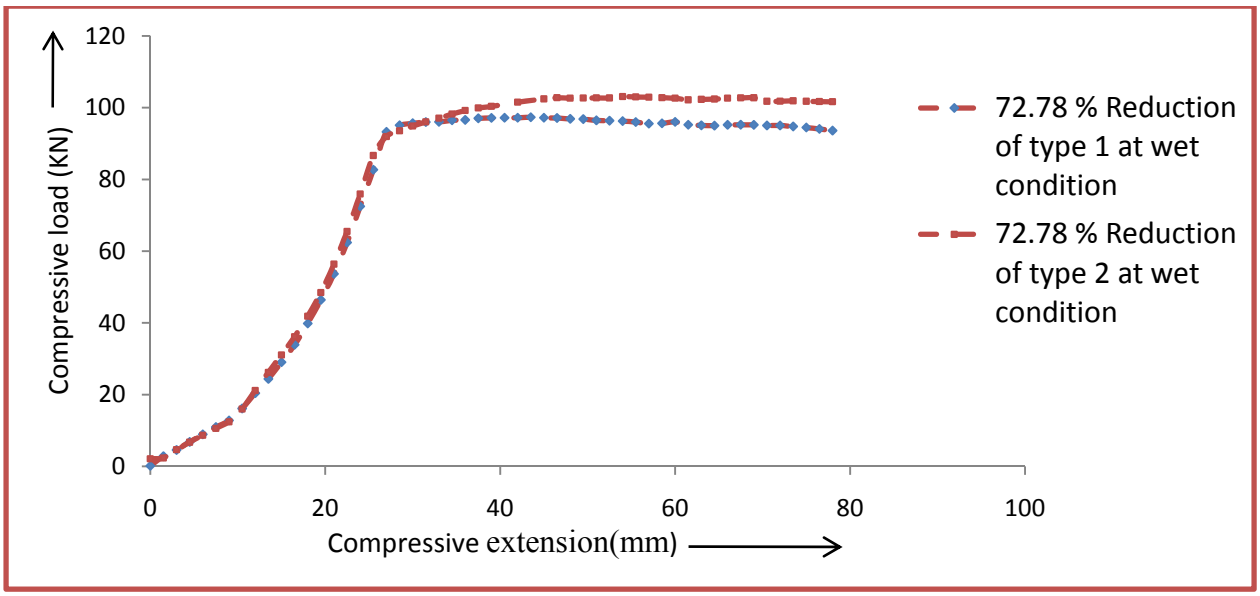

Fig 4.16 Variation of Compressive Load with Extension at Wet Condition

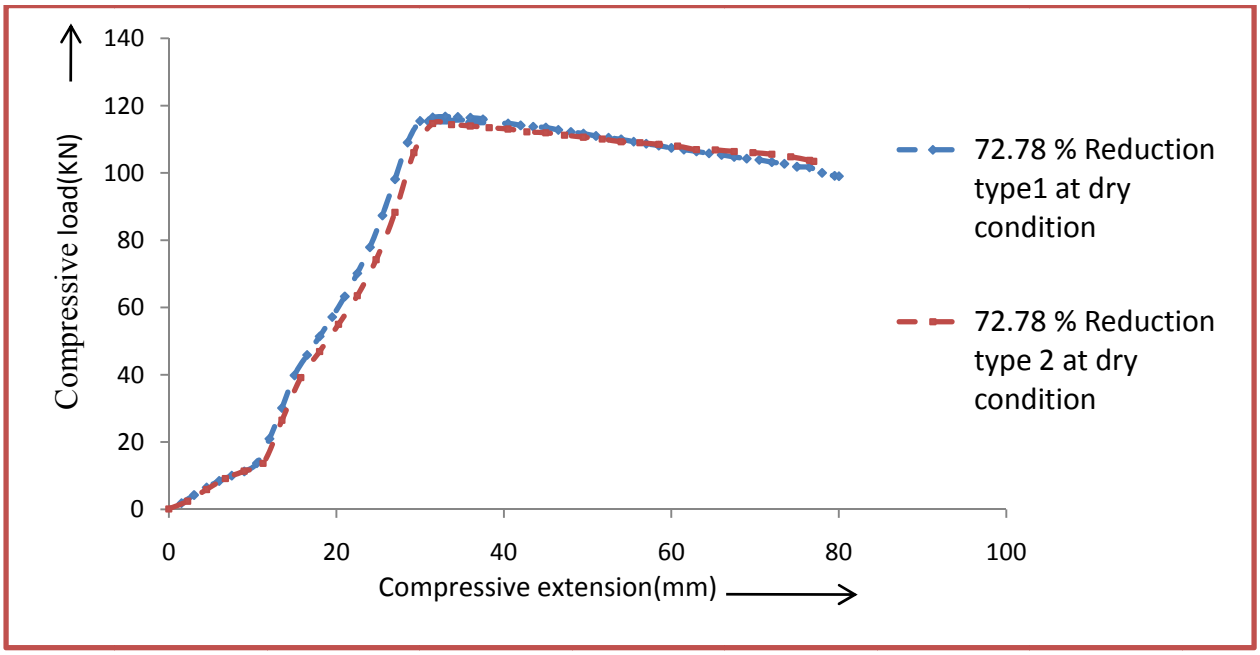

Fig 4.17 Variation of Compressive Load with Extension at Dry Condition

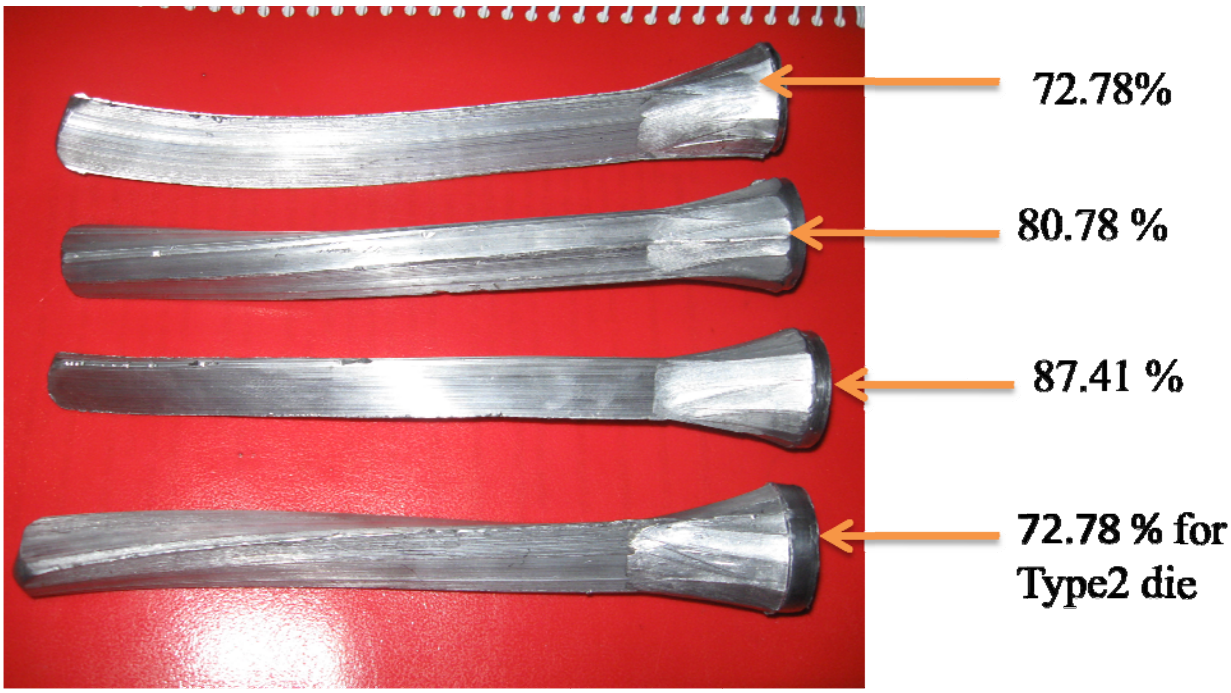

Fig 4.18 Photograph Extruded product at wet condition

Fig 4.19 Photograph of Extruded product at dry condition

Fig 4.20 Photograph of Shape of product inside die

TABLE. 4.2

Experiment results

Experiment	%Red	Friction Factor	ε Strain	Load F (KN)	Pavg (KN/m^2)	σ_0 (KN/m^2)	P_{avg}/σ_0	Eqvt.cone Angle
1. type 1 dry	72.78	0.76	2.75	109.9560	145683	25560	5.69	21.12
2. type 1 dry	80.78	0.76	3.28	132.7793	175922	25560	6.80	24.66
3. type 1 dry	87.41	0.76	3.908	147.340	195214	25560	7.63	28.18
4 .type 2 dry	72.78	0.76	2.75	104.3480	151502	25560	5.61	21.12
5. type 1 wet	78.78	0.38	3.28	90.041	119297	25560	4.99	21.12
6. type 1 wet	80.78	0.38	3.28	103.52	137156	25560	5.36	24.66
7. type 1 wet	72.78	0.38	3.908	124.01	164290	25560	6.42	28.18
8. type 2 wet	72.78	0.38	2.75	89.76	118925	25560	4.65	21.12

Area of billet $(A_b) = (\pi/4).(D_b)^2$

$= (\pi/4)(31)^2$

$= 754.76\ mm^2$

$P_{avg} = (F/A_b)$

TABLE 4.3

Theoretical result of non-dimensional extrusion pressure

%Red	Friction Factor	Eq. Semi cone Angle	P_{avg}/σ_0 (Theoretical)	P_{avg}/σ_0 (Experimental)	Error
72.78	0.76	10.56	5.72	5.69	0.52 %
80.78	0.76	12.33	6.51	6.80	-4.45 %
87.41	0.76	14.09	7.65	7.63	0.26 %
72.78	0.38	10.56	4.69	4.99	-6.39
80.78	0.38	12.33	5.38	5.36	0.37 %
87.41	0.38	14.09	6.45	6.42	0.46 %

4.6 Result and Discussion

The variation of compressive load with extension was determined from the extrusion test for TRIANGULAR cross section taper dies shown in fig4.12. Referring to the Figs 4.13, 4.14, 4.15, 4.16 and 4.17 seen that a typical diagram consists of two stages; namely

(1) A coining stage in which load increases gradually and reaches peak value due to initial compression of billet.

(2) A steady stage of extrusion in which load maintains approximately a constant value upto the end of the extrusion.

The average load corresponding to the second stage consider as the extrusion load. The value of uniaxial yield stress in compression σ_0 , is calculated from stress strain characteristics plot of lead and non- dimensional mean extrusion pressure (P_{avg}/σ_0) is calculated.

Referring to Figs 4.13, 4.14, 4.15, 4.16 and 4.17 the extrusion load decreases marginally with punch displacement for lubricated condition during steady state stage, but it is more prominent for dry condition. This may be attributed to the high friction exist between billet and container in dry condition, which decreases with the length of the billet. In case of type 2 die the requirement of load for same reduction the load is marginally in dry condition but prominent in wet condition. In case of type 2 die the requirement of load for same reduction the load is more as compared to type 1 die in wet condition .This may probably due to decrease of work hardening of material by changing the direction of flow.

The comparison of experimental values with that of theoretical results shows the error remains within 10 percent.

CHPTER FIVE

CONCLUSION & FUTURE WORKS

CHAPTER 5

5.1 CONCLUSION

From the present study the following conclusions may be drawn:

- The upper bound analysis of extrusion of different sections taper dies can carry out by using discontinuous velocity field (modified SERR technique). These techniques provided a better method of analysis for this type of section extrusion, which are difficult by the continuous velocity field formulation.
- Increasing the percentage of reduction accompanying with increase in extrusion loads.
- Using this solution, the optimal die geometry (equivalent semi-cone angle) can be obtained for different area reductions and friction conditions.
- Comparison made with existing theoretical and experimental results shows that the present solution can predict reasonable upper-bound extrusion pressure.
- The present method can be extended to obtain the solution of generalized problems of non-axisymetric extrusion or drawing through taper dies.

5.2 FUTURE WORKS

1. Theoretical prediction of non-dimensional extrusion pressure for different formulationlike triple point formulation.

2. Experimental validation for the different shapes **(**L-Section. Channel section).

3. Equivalent semi cone angle compared with experimental and identified the optimum one.

REFFERNCES

REFERENCES

[1] V. Nagpal, T. Altan, Analysis of the three-dimensional metal flow in extrusion of shapes. With the use of dual stream function, in: Proceedings of the Third North American Metal Research Conference, Pittsburgh, PA, 1975, pp. 26–40.

[2] B.B. Basily, D.H. Sansome, Some theoretical considerations for the direct drawing of section rod from round bar, Int. J. Mech. Sci. 18 (1979) 201–209.

[3] D.Y. Yang, C.H. Lee, Analysis of three-dimensional extrusion of sections through curved dies by conformal transformations, Int. J. Mech. Sci. 20 (1978) 541–552.

[4] W. Johnson, H. Kudo, The Mechanics of Metal Extrusion.(1963)

[5] Hill, Analysis metal working process, mechanics of physical solids flow rule(1963)

[6] R. Prakash, O.H. Khan, An analysis of plastic flow through polygonal converging dies with generalised boundaries of the zone of plastic deformation, Int. J. Mach. Tool Des. Res. 19 (1979) 1–9.

[7] F. Gatto, A. Giarda, The characteristics of three-dimensional analysis of plastic deformation according to the SERR method, Int. J. Mech. Sci. 23 (1981) 129–148.

[8] P.K. Kar, N.S. Das, Upper bound analysis of extrusion of I-section bars from square:rectangular billets through square dies, Int. J. Mech. Sci. 39 (8) (1997) 925–934.

[9] P.K. Kar, R.K. Sahoo, Application of the SERR technique to the analysis of extrusion of sections from round billets, J. Inst. Engrs. (India) 78 (1997) 15

[10] S.K. Sahoo, P.K. Kar , K.C. Singh a. A numerical application of the upper-bound technique for round-to-hexagon extrusion through linearly converging dies,Int. J. Mat. Pro. Tec. 91 (1999) 105–110

[11] Narayanasamy R, Ponalagusamy R, Venkatesan R, Srinivasan P (2006) An upper bound solution to extrusion of circular billet to circular shape through cosine die. Mater Des 27(5):411–415. doi:10.1016/j.matdes.2004.11.026

[12] J.S. Gunasekera, S. Hosino, Analysis of extrusion or drawing ofpolygonal sections through straightly conversing dies, J. Engng. Ind.Trans. ASME 104 (1982) 38–43.

[13] C.B. Boer, W.R. Schneider, B. Avitzur, An upper bound approach forthe direct drawing of square section rod from round bar, in: Proceedings of the 20th International Machine Tool Design and Research Conference, Birmingham, 1980, pp. 149–155

[14] D.Y. Yang, M.U. Kim, C.H. Lee, A new approach for generalized three-dimensional extrusion of sections from round billets by conformal transformation, IUTAM Symp. Metal Forming Plasticity, Germany, 1979, pp. 204–221.

[15] B, Vvitzur, Metal forming process and analysis, capter10 (1977)

[16] Geoffrey W. Rowe, Introduction to the principle of metal working, Chapter-8

[17] V. Gopinathan, Plasticity Theory and its Application in Metal Forming, Chapter 7